ACTINIDE RESEARCH QUARTERLY

89 Ac | 90 Th | 91 Pa | 92 U | 93 Np | 94 Pu | 95 Am | 96 Cm | 97 Bk | 98 Cf | 99 Es | 100 Fm | 101 Md | 102 No | 103 Lr

First Quarter 2015

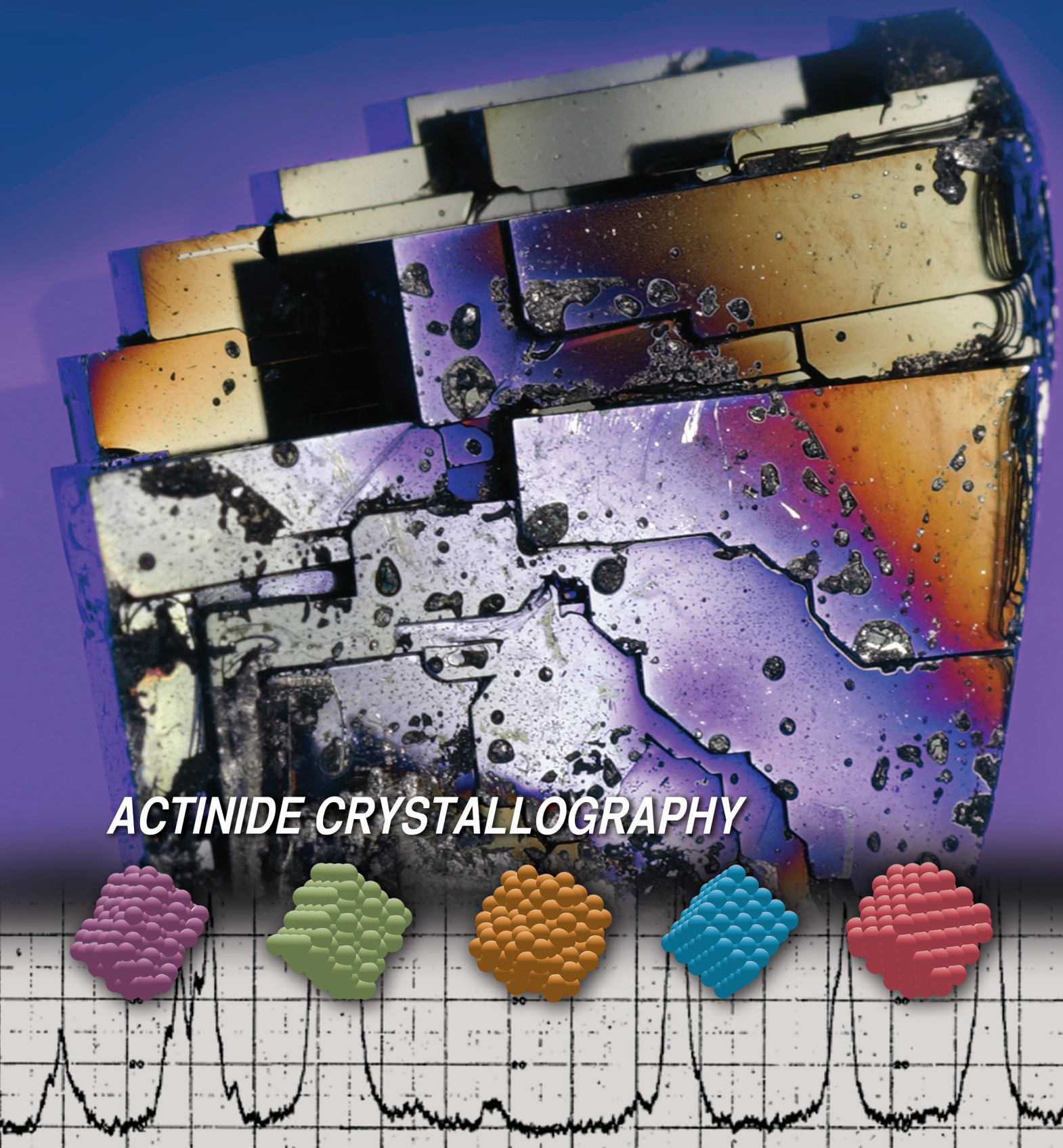

ACTINIDE CRYSTALLOGRAPHY

About the cover

The crystalline structure of plutonium in its elemental form, and in molecules and compounds with other elements, is the basis for understanding the intriguing chemistry, physics, and engineering of plutonium molecules and compounds. Colored balls stacked according to the given crystalline symmetry of the five solid allotropes of plutonium are shown, left to right: α (monoclinic), β (body-centered monoclinic), γ (face-centered orthorhombic), δ (face-centered cubic), and ε (body-centered cubic). The graph is the original diffraction pattern for elemental plutonium. The background image is a $PuCoGa_5$ single crystal with an underlying tetragonal symmetry that exhibits the unique electronic property of superconductivity associated with this symmetry.

The Seaborg Institute welcomes Brian L. Scott as guest editor for this special Actinide Research Quarterly issue showcasing the rich science and history of the crystallography of actinides. A staff scientist at Los Alamos National Laboratory, Brian has extensive experience in structure determination using single-crystal and powder x-ray diffraction techniques. He has explored molecular and solid-state structures in a variety of materials ranging from bioinorganic molecules to plutonium-based superconductors. His interests include structural inorganic chemistry and the synthesis and characterization of actinide-containing materials important to understanding f-orbital bonding and reactivity. He has authored over 350 papers, with more than 8,000 citations.

FROM THE GUEST EDITOR

The year 2014 was the UNESCO International Year of Crystallography.

In 1611, Johannes Kepler speculated that snowflakes were hexagonal grids of water molecules, but it wasn't until the discovery of x-rays almost 300 years later that this theory could be tested. In 1913, William Henry Bragg and his son William Lawrence Bragg discovered that regular arrays of atoms and their subsequent patterns of electron density in crystals diffract x-rays in a way that made it possible to determine the three-dimensional arrangement of atoms in crystals. They applied this technique to diamond, showing that the tetrahedral coordination geometry of carbon predicted for decades was indeed correct. For this work they were awarded the 1915 Nobel Prize in physics. Since then, x-ray diffraction has become a fundamental tool for chemists and biochemists, materials scientists, and physicists because a three-dimensional crystallographic structure provides an intellectual framework to connect chemical structure to physical properties. Twenty-eight Nobel Prizes have been awarded for advances in x-ray diffraction or for research that relied on x-ray diffraction as a crucial part of the work.

The rich history of crystallography at Los Alamos began in the 1940s and continues today. This issue focuses on the crystallographic structures of materials containing actinides. X-ray crystal structure data reside in two international databases: The Cambridge Structural Database (CSD), which stores structural data of molecules having at least one hydrogen and one carbon; and the Inorganic Crystal Structure Database (ICSD), which contains mostly metals and alloys. Los Alamos has contributed more than 300 actinide-containing structures to the CSD and more than 100 to the ICSD for materials ranging from alloys to molecular solids.

The actinide work described herein is deeply rooted in understanding bonding and reactivity of the *f* electrons. The chemistry presented is intended to appeal to a broad audience, generally keeping to basic ideas such as Lewis acids and bases, hard-soft donor acceptor theory, and covalency while showcasing how our understanding of actinide chemistry continues to evolve in important ways.

The physics, chemistry, and materials science presented range from plutonium-based superconductors to plutonium molecules that have potential applications to nuclear waste remediation. But even for the non-expert, I hope the natural symmetry of the crystallographic structures is enchanting in and of itself.

Brian L. Scott

Guest Editor

Address correspondence to

Actinide Research Quarterly
c/o Editor
Mail Stop T-001
Los Alamos National Laboratory
Los Alamos, NM 87545

ARQ can be read online at

www.lanl.gov/arq

If you have questions, comments, suggestions, or contributions, please contact the ARQ staff at
arq@lanl.gov or (505) 665-0858

Los Alamos National Laboratory
National Security Education Center

David L. Clark, Director

Glenn T. Seaborg Institute

Albert Migliori, Director
Franz Freibert, Deputy Director

Actinide Research Quarterly

Publication Coordinator
Susan Ramsay

Guest Editor
Brian L. Scott

Science Advisors
Albert Migliori
Franz Freibert
Jaqueline Kiplinger

Editors
Sue King
Susan Ramsay
Amy Reeves
Octavio Ramos Jr.

Designers/Illustrators
Kelly L. Parker
Barbara V. Maes

Copy and Print Proofing Editors
Susan M. Ramsay
Amy Reeves

Printing Coordinator
Alexandria M. Salazar

Circulation Manager
Susan Ramsay

In this issue

A History of Crystallography at Los Alamos, 1951–1994

This article was contributed by Brian L. Scott, Materials Physics and Applications Division, Los Alamos National Laboratory, guest editor of this issue; and Bob Ryan, Los Alamos National Laboratory, retired, whose work is covered in this article.

During his 37-year career at Los Alamos National Laboratory, Bob Penneman took on many roles, including deputy group leader, group leader, and most importantly, intellectual and visional leader of the Inorganic Chemistry Group.

Founded and given the code name Site Y in early 1943, Los Alamos became Los Alamos Scientific Laboratory in 1945 and Los Alamos National Laboratory in 1981.

The Beginnings

The crystal structure of plutonium was of great interest during the Manhattan Project, but the first crystallographer at Los Alamos Scientific Laboratory was most likely Finley H. Ellinger, who initially contributed to "The Nickel-Plutonium System," published as classified report LA-1304 in March 1951. This work identified several new plutonium-nickel phases and their lattice constants based on powder and single-crystal data. Ellinger collaborated extensively with the famous crystallographer Willie Zachariasen from the University of Chicago. Zachariasen frequently travelled to Los Alamos to visit friends in the early fifties and began collaborations in the summers with Bob Penneman and other scientists in the Inorganic Chemistry Group, including Ellinger. Penneman was largely responsible for building the Inorganic Chemistry Group at Los Alamos, which came to be regarded as one of the premier inorganic chemistry groups in the world, and crystallography laid the structural foundation for much of this group's research.

Zachariasen retired to Santa Fe in the seventies and continued to collaborate with inorganic chemists at Los Alamos. Together Zachariason and Ellinger would go on to publish numerous structures of plutonium, americium, curium, and related intermetallic systems.

The most notable of these structural studies of the fifties and early sixties are the solutions of the crystal structures of the α, β, and γ phases of plutonium, which at that time were a longstanding problem. The art and science of converting a set of Bragg reflections into a 3D structure is known as "solving the structure." This task is greatly complicated by the so-called phase problem in x-ray diffraction. Both the amplitude of the Bragg reflection and the phase relation to other reflections in the data set are needed to determine the atomic positions in the unit cell. The intensity amplitudes could be measured using photographic or x-ray detectors, but to this day the phasing information remains unmeasurable. Remarkably, Zachariasen employed his phenomenal crystallographic intuition to solve the structures of these three phases of plutonium. Methods of calculating phase probabilities to narrow down a myriad of potential structure solutions had not yet been developed. His scientific achievement is described in the article in this issue by Albert Migliori and Franz J. Freibert, "Reflections of Plutonium—in Search of Solutions to a Difficult Crystallography Problem."

The crystallographers Don T. Cromer and Allen C. Larson came to Los Alamos in the mid-fifties and continued to publish papers well into the 1980s. In 1957, Cromer, Larson, and Stambaugh published the crystal structure of the plutonium-aluminum intermetallic compound, $PuAl_3$. In general, it is much easier to solve a crystal structure from single-crystal data because the reflections are resolved in three dimensions, whereas in a

powder pattern the reflections are piled up along a one-dimensional axis and must be deconvoluted. Thus, the establishment of single-crystal capability at Los Alamos was an important one, and this was the first crystal structure to be determined from a single crystal at Los Alamos. At that time, the x-ray reflection data were collected using photographic film. To solve the $PuAl_3$ structure, 319 reflections were indexed and intensities estimated by eye from the photographs. This crystal structure and others published in the fifties and early sixties at Los Alamos focused mainly on the phases of plutonium and its alloys and compounds.

The 1960s to 1990s

There was a worldwide renaissance in x-ray crystallography in the 1960s, and Cromer and Larsen were at the forefront of these efforts. During that time, Cromer developed the Laboratory's first fully automated diffractometer, which relieved the investigator of many boring and painstakingly tedious hours in the data collection process. Automated diffraction greatly reduced the need for photographic work through counting or measurement of reflection intensities using x-ray detectors and goniometers to drive the crystal and detector to the positions required to achieve diffraction. At that time, the atomic scattering factor, which is a measure of the scattering power of an isolated atom, had not been adequately developed for heavy atoms ($Z > 37$) because of relativistic effects. Accurate scattering factors are crucial in determining the intensities and phases needed to calculate structure factors based on crystal structure models.

Least-squares refinement of the structural model minimizes the difference between the calculated and measured structure factors using atomic positions and temperature factors as the fitting parameters. Cromer and others employed self-consistent-field Dirac-Slater wave functions to make relativistic calculations on these heavy atoms and ions. These values are still used by crystallographers worldwide and appear in the *International Tables for Crystallography*, the definitive reference published by the International Union of Crystallography.

In the sixties, as counting devices began to replace photographic methods, the effects of anomalous dispersion could be measured. Once again Cromer performed relativistic calculations to produce an anomalous dispersion correction to the scattering factors, and these also appear in the *International Tables* to this day. As a result of Cromer's work, he became the most referenced author in the chemical world and received a coveted E. O. Lawrence award in 1969.

Concurrent with Cromer's work, Al Larson was developing software and automated techniques for collecting, analyzing, and refining x-ray diffraction data. Larson's programming efforts had greatly enhanced the solution and refinement capabilities of those interested in structural chemistry. For example, programs available at that time required the entry of many lines of information defining the symmetry-related positions of atoms in the crystal, a time-consuming and error-prone process, whereas Larson had programmed in the capability to generate this information from the space group symbol that could be entered in seconds. In another example, the solution of

"There was a worldwide renaissance in x-ray crystallography in the 1960s."

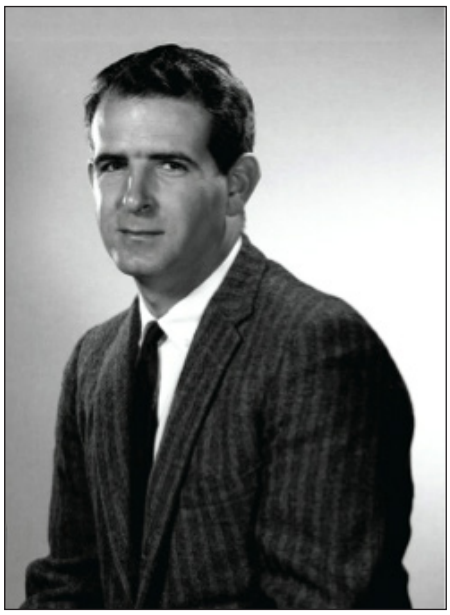

Bob Ryan performed chemical structure studies on a variety of chemical systems at Los Alamos for more than 20 years in the late 1960s, 1970s, and into the 1980s.

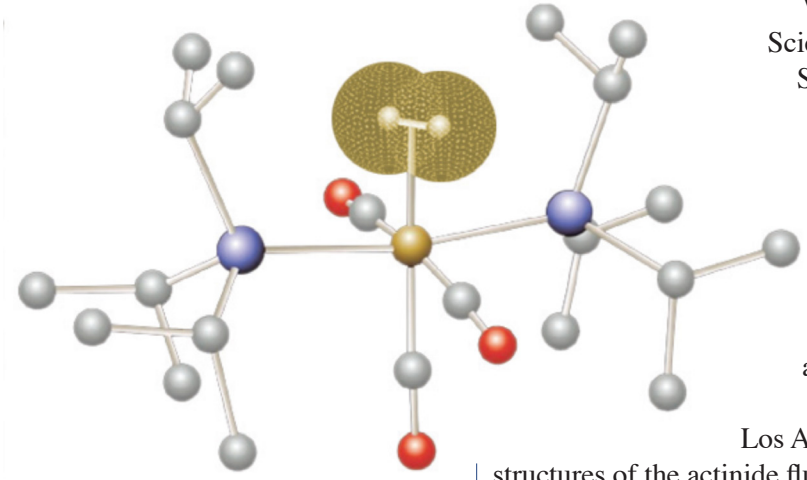

Kubas' dihydrogen complex showing two hydrogen atoms (in brown electron cloud) bonded to tungsten (gold sphere) to form a new metal-ligand complex. Blue spheres are phosphorus, red spheres are oxygen, and gray spheres are carbon.

structures with atoms of comparable scattering power had only recently become possible through the "direct methods" developed by Karle and Hauptman (who shared the Nobel Prize in chemistry for this work in 1985), and Larson included these algorithms in his software. These developments allowed structures to be solved overnight at Los Alamos, while others were still manually solving structures over the course of several days.

When Bob Ryan arrived in 1967 from a National Science Foundation post-doc position in the Zurich, Switzerland labs of the prominent crystallographer Jack Dunitz, Ryan realized the power of what Larson and Cromer had created at Los Alamos: "The stage was set then when I arrived for a greatly accelerated production of structural information which provided a solid foundation for much of the chemical progress that ensued from Penneman's group over the next 25 years and beyond."

Bob Ryan's first crystallographic project at Los Alamos Scientific Laboratory focused on the structures of the actinide fluorides, which was motivated by their importance in the nuclear weapons and energy arenas. This research spanned 20 years and was reviewed by Ryan, Penneman, and Rosenzweig in 1973 in the journal *Structure and Bonding*. The x-ray structures from this work were pivotal to understanding the coordination chemistry of the actinides as well as relationships between actinide valence and ion sizes.

Greg Kubas, a very capable chemist with outstanding creative vision, arrived at Los Alamos not long after Ryan, and they formed a long-lasting collaboration. Kubas' initial charge was to explore the chemistry of SO_2, a subject of national concern at the time because of the acid rain issue, and he began by studying the interaction of SO_2 with transition metal complexes. sulfur dioxide exhibits an amphoteric interaction, which is a clear indicator of the nature of the bonding between the ligand and metal complex fragment. This technical challenge provided fertile ground for an extended program that explored the structure and bonding interplay along with the attendant chemistry. Kubas' research showed that SO_2 bonded to metals in more different ways than any other ligand. Ryan's crystallographic studies were key to understanding the structure and bonding in these systems. As a serendipitous bonus of Kubas' work, while exploring the possibility of catalytic reactivity between SO_2 and hydrogen in the presence of the many complexes Kubas synthesized, an entirely new type of complex was isolated. This new type of metal-ligand complex was shown to be the first example of a transition metal complex containing molecular hydrogen as a ligand.

Ryan determined the x-ray structure, while Phil Vergamini performed the neutron study at the Los Alamos Meson Physics Facility to accurately locate the hydrogen atom positions. Although this structure does not contain an actinide metal, the structure and commensurate chemistry held great interest as the first structural example of how hydrogen interacts with a metal.

These findings were relevant to future hydrogen-actinide interactions of interest at Los Alamos. This discovery was heralded as the most important in inorganic chemistry in the previous two or three decades and catapulted Kubas to instant fame and recognition, including a 1994 E. O. Lawrence Award.

With the discovery of uranocene in the late sixties by Andrew Streitweiser, the study of actinide organometallic complexes was underway. The first organoactinide complex structurally characterized at Los Alamos was determined by Ryan from crystals provided by Penneman's collaborator, Basil Kanellakopulos, in 1975. The complex $U(Cp)_3F$, presented a challenge crystallographically in that the Cp (cyclopentadienyl, C_5H_5) rings were rotationally disordered. A crystal structure is a bulk measurement, and is the average of every unit cell in the crystal. Thus, if the Cp has different positions in each unit cell, then when averaged, an untidy mess is presented to the crystallographer, who must deconvolve the integrated electron density to arrive at the true structure. This disorder problem with Cp and also its methylated cousin, $Cp^* = C_5Me_5$, would plague crystallographers for years in the determination of organometallic structures. The study of organoactinide complexes increased dramatically in ensuing years with the chemistry of Al Sattelberger, Dave Moody, Carol Burns, and their collaborators. From a structural point of view, the most noteworthy results were perhaps the structures of $Th(C_5Me_5)_2(\mu\text{-}PPh_2)_2Ni(CO)_2$ and subsequently $(C_5Me_5)_2Th(\mu\text{-}PPh_2)_2Pt(PMe_3)$, both published in the eighties.

Both of these complexes show metal–metal distances that are significantly shorter than expected for a non-bonding contact and are the first examples of metal–metal bonding between an actinide and a transition metal. Organoactinide chemistry continues to be an advancing area of study at Los Alamos today. Hundreds of crystal structures published in diverse areas in the fifties and into the nineties at Los Alamos built the foundation for understanding structure, bonding, reactivity, and other properties in actinide materials ranging from pure metals to organoactinide complexes. Books and book chapters have been written on the research performed during this time at Los Alamos, demonstrating a breadth of the chemistry and commensurate chemical structure greater than can be captured in this article. Crystallography was established at Los Alamos in the infancy of actinide science. It took people like Finley, Zachariasen, Cromer, Larson, and Ryan to take very new scientific ideas and put them into practice. The literature shows that they were clearly successful, and they laid the groundwork for the current state of actinide crystallography.

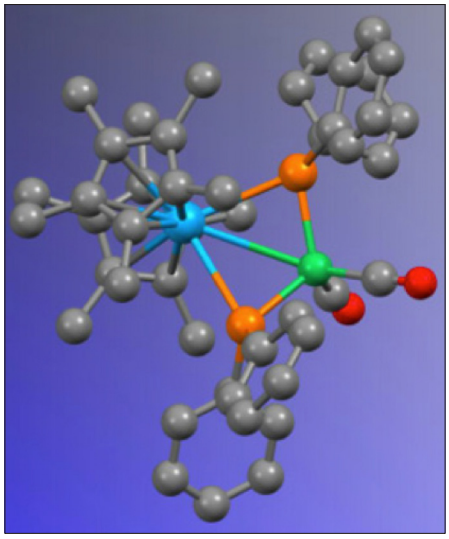

The structure of the organoactinide complex $Th(C_5Me_5)_2(\mu\text{-}PPh_2)_2Ni(CO)_2$, shown here with thorium (blue), nickel (green), oxygen (red), phosphorous (orange), and carbon (gray), was one of hundreds of organometallic structures published as a result of the research at Los Alamos that laid groundwork for the current state of actinide crystallography.

The Present and Future of X-Ray Crystallography at Los Alamos

This article was contributed by the guest editor of this issue, Brian L. Scott, Materials and Physics Applications Division, Los Alamos National Laboratory.

The three scientists who established single-crystal x-ray diffraction at Los Alamos Scientific Laboratory during the sixties, seventies, and eighties had all retired by the early nineties. The contributions of Don Cromer, Al Larson, and Bob Ryan are described in the first article of this issue, "A History of Crystallography at Los Alamos, 1951–1994." Because I was hired in 1994 as the crystallographer in the Los Alamos Inorganic Chemistry Group, INC-4, I did not have the opportunity to work with them. However, their legacy remained.

In 1994, INC-4 had two fully automated diffractometers with photomultiplier tube (PMT) detectors and sealed-source x-ray tubes. There was also a precision camera for aligning crystals for magnetism and optical spectroscopy experiments. The PMT detectors were interfaced to scintillator crystals to convert the diffracted x-ray photons into light that the PMT detectors could detect and convert to electrical signals to complete the measurement. These PMT detectors had been the workhorse of single-crystal x-ray diffractometers for the past two decades, and were certainly a huge improvement over having to estimate reflection intensities from photographic film.

Still, the PMT detectors left a lot to be desired. They could only measure one reflection at a time and for most structures required thousands or even tens of thousands of reflections. Data collection could take up to a week or more. Crystals were carefully screened before data collection using photographic film techniques to ensure valuable diffractometer time was not wasted on poor crystals. Also, time had to be spent before data collection carefully determining the orientation of the crystal axes so the PMT and crystal could be driven to the precise location for each reflection. Setting up a data collection could take half a day, but was worth the time to ensure one was not collecting a day's worth of data on a twinned crystal, which often resulted in data sets that couldn't be solved to yield a structure.

In the mid-nineties, Siemens developed the charge-coupled device (CCD), a detector for imaging x-ray reflections, which revolutionized the field. This is the same CCD technology currently used in most digital cameras, and at that time the detector was built around a 1-cm^2 CCD chip. The detector face was an approximately 6-cm-diameter scintillator crystal interfaced to a tapered fiber-optic bundle that demagnified the scintillations down to the 1-cm^2 CCD crystal where the light was imaged. This was a great improvement over the PMT technology because many reflections could be imaged at once, with each set of reflections being collected much faster than a single PMT reflection. As a result, data collection times dropped from three to seven days to just one day.

Moreover, the CCD chips were much more sensitive to light than PMT detectors, which afforded much higher quality data, resulting in more accurate

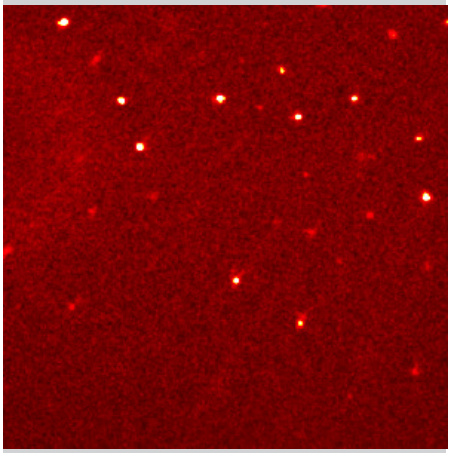

CCD image of x-ray diffraction from a single crystal. Each spot represents a Bragg reflection. Imaging many reflections at once enables much shorter data collection times than were possible with the earlier PMT detector technology.

measurement of bond distances and angles. Perhaps the greatest advantage was the ability to measure much smaller crystals; the size of crystal that could be used for structure determination dropped by half. PMT detector-based systems required crystals to be on average 0.40–0.50 mm in their smallest dimension. This dropped to just under 0.20 mm with the advent of the CCD. The ability to characterize smaller crystals opened the door to collecting numerous structure results that were not previously obtainable. The subsequent visualization software, coupled with speed of data collection, allowed crystal quality to be assessed rapidly, reducing the crystallographer's time for setting up a data collection from hours to minutes. In 1998, Los Alamos obtained its first CCD which greatly improved the quality and number of actinide crystal structures coming out of Los Alamos.

Soon after I was hired, Dave Clark expressed interest in performing structure determinations on crystals containing transuranic elements. Because of increased safety and health regulations, this capability had fallen by the wayside in the seventies and eighties. Clark, Phil Palmer, and I collaborated to develop a containment system that would mitigate the health hazards of working with transuranic elements outside of a fume hood or glovebox, while at the same time allowing x-rays into and out of crystalline samples. Clark had learned that a German group was using a triple containment technique that consisted of thinly coating the crystal with epoxy, placing the crystal in a quartz capillary and sealing the ends, and then coating the capillary with a thin layer of acrylic to prevent dispersal if the capillary were cracked.

Scientists use a triple containment technique that consists of four stages to prepare crystals to determine their structures with the use of CCD technology. From left to right are a crystal mounted on glass fiber, a crystal on glass fiber inside a capillary, a capillary coated with acrylic, and a crystal contained after breakage of a capillary.

For our work, the triple containment technique had to result in a sealed crystal without radioactive contamination on the surface of the acrylic-coated capillary. The work was greatly complicated by the small size of the crystal (<0.6 mm) and because it had to be done in a glovebox. Finally, Clark and Palmer were successful in delivering a cleanly sealed crystal to me, and I decided whether the signal-to-noise ratios resulting from the attenuated x-rays and increased backgrounds from the containment materials would be sufficient to determine a structure.

The first set of structures to be determined using the triple containment technique were the quanidinium salts of $AnO_2(CO_3)_3^{4-}$ with An = Pu or Np. To observe the bonding trends across the actinide series, the corresponding uranium structure was determined as well.

When the structures were solved and refined, we noticed that the An=O distances did not trend properly from uranium to neptunium to plutonium.

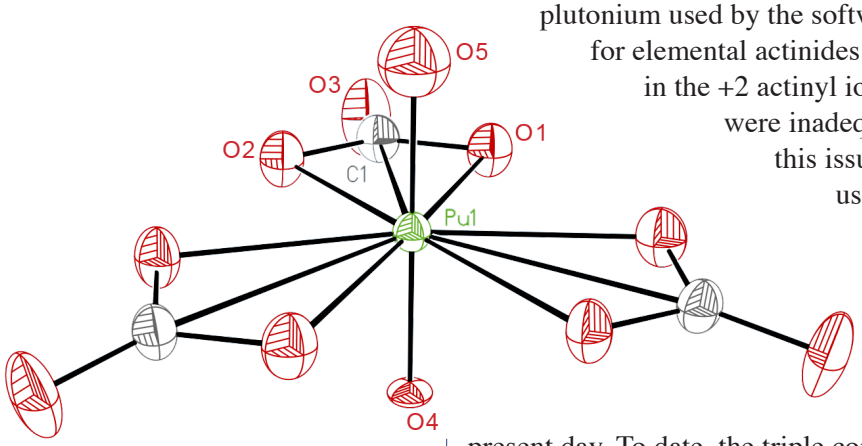

Thermal ellipsoid plot of $[PuO_2(CO_3)_3]^{4-}$, with Pu, C, and O atoms colored as green, gray, and red, respectively. The plutonyl oxygen atoms, O4 and O5, have distinctly different temperature factors consistent with the asymmetric O=Pu=O geometry.

Instead of showing the expected decrease, the An=O bonds showed a slight increase in distance. An investigation of the atomic scattering factors for plutonium used by the software refinement program showed values for elemental actinides. Because the valence state of the actinide in the +2 actinyl ions is +6, the elemental scattering factors were inadequate. As mentioned in the first article in this issue, Don Cromer had calculated these values using relativistic techniques 30 years before. A correction of the scattering factors to Cromer's values yielded the proper bonding trends. After these first studies, Cromer's values were used for the actinides, which demonstrates that the impact of his work continues to the present day. To date, the triple containment technique has allowed several hundred transuranic structures to be determined, and Los Alamos is a world leader in the synthesis and structural determination of transuranic materials.

The CCD technologies continued to advance. In the early 2000s, the x-ray detector technology was improved significantly. Instead of the 1-cm^2 chip of the first generation of detectors, the new chips were 6 cm^2, which eliminated the need for the fiber-optic taper. These advances, along with new readout techniques, made the new detectors much faster. The new dectectors were also much more sensitive, and the required crystal size dropped further to 100 microns. The small sizes of crystals, which were traditionally mounted on glass fibers, required a new mounting system. A trick was borrowed from protein crystallography: the crystal was scooped up in a nylon loop and suspended in a thin film of perfluorinated oil.

The accuracy of measurement of bond distances and angles increased as well. Los Alamos acquired one of these second-generation systems in 2005, and this instrument is still in use. With increased detector speed and intensity, a full data set can be collected in two to six hours, depending on crystal quality and symmetry. Along with improved data quality, the ability to solve twinned structures in a more timely fashion was realized. Before the advent of CCD technology, resolving twinned structures was very time consuming, and required trial and error, photographic work, and additional data collection time to collect reflections from the second twin component. Because the CCD face is pixelated and active over its entire surface area, data on twinned reflections are collected as well. The new technology makes it relatively easy to index, integrate, and refine all components of a twinned structure. Because some crystal systems only grow as twins, this has opened the door to previously unobtainable characterization of structures. Finally, in addition to traditional direct methods and Patterson's techniques for solving crystal structures, charge-flipping algorithms (CFAs) have been introduced as a technique for solving hard-to-crack structures. Use of CFAs is a dual-space technique that uses fundamental electron density relationships in crystals and has allowed the solution of structures when traditional methods fail.

Typically the crystals are cooled during data collection for two reasons. The first is that low-temperature data sets are of higher quality because of the decreased thermal motion of the atoms in the crystal, resulting in higher reflection intensities. The second is that many crystals are air sensitive, and cooling to temperatures as low as 120 K keeps them chemically stable. Traditionally, crystals were cooled using a liquid-nitrogen stream created from controlled boil-off in a cryogenic Dewar flask. In 2008, Los Alamos scientists began using a closed-cycle nitrogen refrigerator that made nitrogen on an as-needed basis, eliminating the costs and effort of dealing with liquid nitrogen. Data collection on transuranic crystals in capillaries is also carried out under cold streams to prevent crystal degradation. One problem with the capillary method is that for air-sensitive crystals the final steps of the procedure occur outside of the glovebox and crystals often decompose during the process. Andrew Gaunt and I are currently working on faster techniques, employing sealed cryoloops to alleviate this problem.

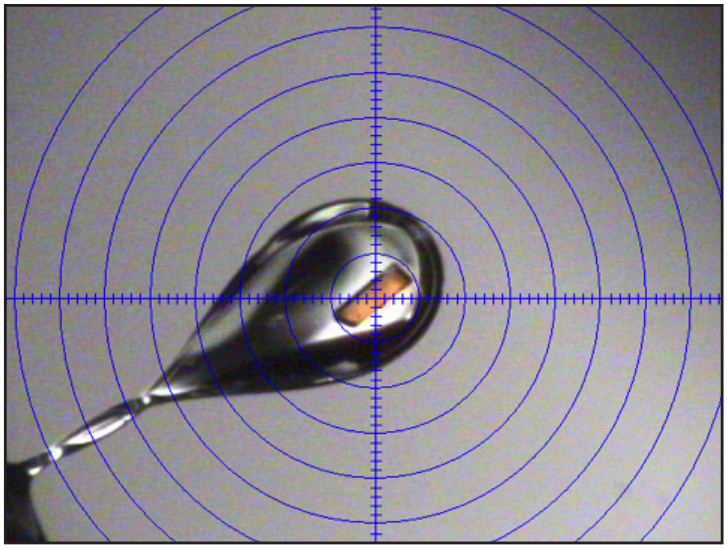

An orange crystal was suspended in a thin film of paratone-n oil in a nylon cryoloop rather than on a glass fiber. The crystal was cooled to 120 K in a liquid-nitrogen vapor stream for CCD characterization. The crystal size is 0.18 x 0.05 x 0.02 mm^3.

The next advances in single-crystal x-ray diffraction have occurred in both detection and x-ray source. The first advance is achieved using a complementary metal-oxide-semiconductor (CMOS) detector, which is larger (100 cm^2 versus 40 cm^2) and provides higher resolution imaging than the CCD now in service at Los Alamos. The second advance is achieved by using a low-power x-ray source that runs at 50 watts and is air cooled; this new source would replace the current 1.5-kW water-cooled x-ray source and represents a ten-fold increase in intensity while using less water and power resources. This x-ray source employs micro-focus, multilayer optics to focus the x-rays, making them very bright and efficient. The ten-fold increase in measured intensity provided by this instrument would allow data collection on crystals an order of magnitude smaller than is currently possible (microns versus tens of microns). Moreover, the increased x-ray flux, when combined with the higher resolution and larger CMOS detector, will result in additional accuracy in measuring bond distances and angles. Higher quality results are needed to keep pace with the ever-increasing need to understand electronic structure and bonding in actinide systems ranging from molecular complexes to extended solids and alloys. The ability to determine defective structures (vacancies, substitutional and positional disorders, and twinning) and superstructure will also increase because of the higher intensity and resolution data sets. Finally, the option to use smaller sample sizes of radioactive materials will provide a safety benefit by reducing the radiation doses to workers. Several divisions at Los Alamos are currently collaborating to purchase a new instrument employing these technologies.

Reflections of Plutonium—

In Search of Solutions to a Difficult Problem in Crystallography

This article was contributed by Albert Migliori, Director, and Franz J. Freibert, Deputy Director, Glenn T. Seaborg Institute for Transactinium Science, Los Alamos National Laboratory.

The original research using x-ray diffraction reflections to determine the crystal structure of plutonium was shrouded by secrecy and classification at Site Y of the Manhattan Project, later to become Los Alamos Scientific Laboratory and then Los Alamos National Laboratory. The rush to make the first plutonium-fueled atomic bomb led to early misconceptions and errors regarding the stunning complexity of the five clearly resolved phases of plutonium, the rarity of plutonium, and the difficulty of working with it.[1] But these issues were resolved well before the structures of plutonium were revealed in peer-reviewed journals years after the work was completed. Eric Jette, a group leader in the Chemistry and Metallurgy Division, in a 1957 peer-reviewed paper with no references[2] wrote, *"The present author is merely acting as a reporter for the work represented in this summary. Since the beginning of 1944, at least forty individuals working in this laboratory have contributed to our knowledge of plutonium metal. Individual reports on the several properties of plutonium will be written by the persons actually concerned with the work today and it is hoped that adequate acknowledgement can be made there of the efforts of the earlier workers. Some time, however, may elapse before these articles can be published and therefore this summary is being presented."*

For example, in January 1945, the wet purification process for plutonium (element 9**4**, atomic weight 23**9**, code-named "49") was tested for the first time at full scale, producing 160 grams of plutonium metal. Using resistivity and dilatometry, Frank Schnettler and his team[1] reconfirmed that plutonium had *five* phases. Yet all this was classified until some

It is interesting to note that in May of 1945, just three months before the Trinity test of the first atomic bomb, the Chemistry and Metallurgy Division minutes included reports of that month's 17 contamination accidents, including two fires and an explosion.[3]

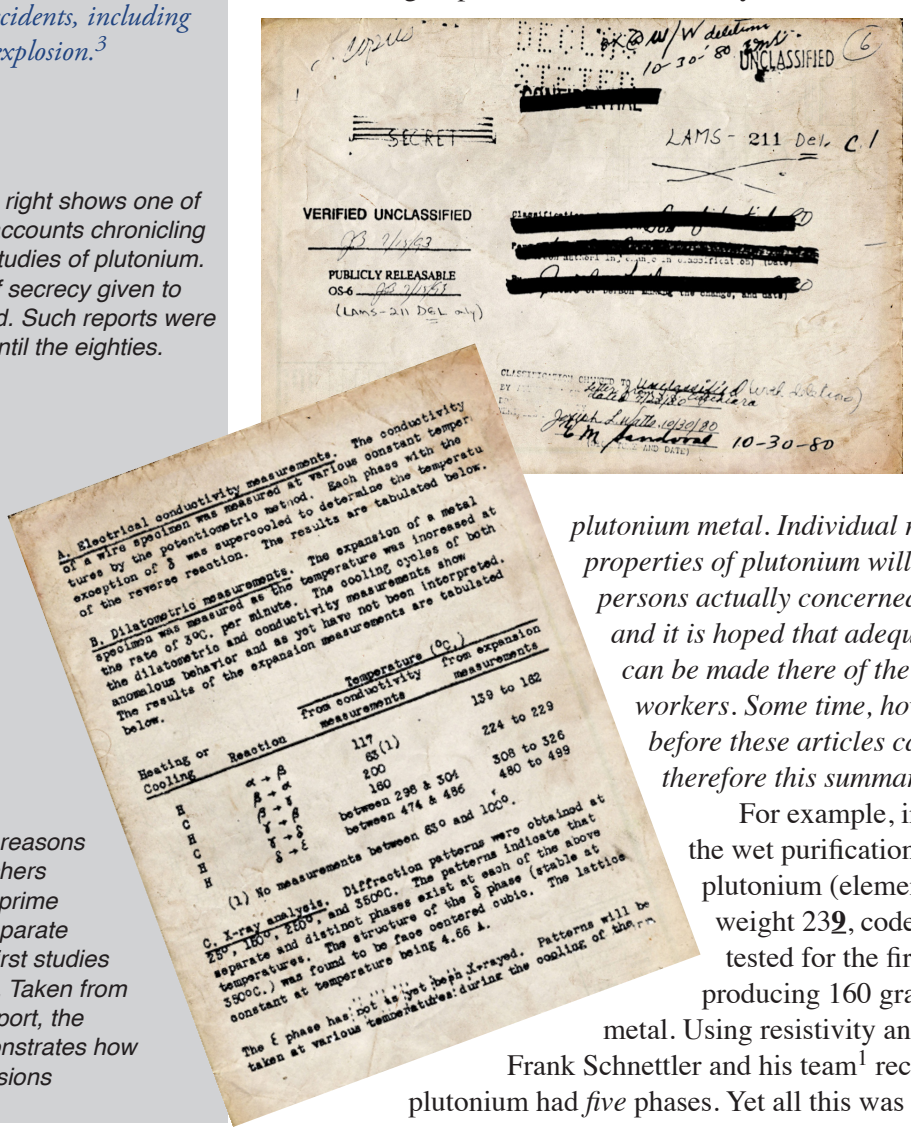

The image on the right shows one of the early written accounts chronicling crystallographic studies of plutonium. Note the extent of secrecy given to reports of this kind. Such reports were not unclassified until the eighties.

There were good reasons as to why researchers did not classify δ-prime plutonium as a separate phase when the first studies were set to paper. Taken from one such early report, the page below demonstrates how erroneous conclusions were reached.

years later when the crystal structures of plutonium in its various zero-pressure phases began to be published.

The creativity involved in solving the crystal structures of plutonium began when Willy (as he insisted on being called) Zachariasen hypothesized that a new series was starting, a series that included elements where active electrons were designated by the symmetry descriptor 5*f*. He gave a talk early in the Manhattan Project, after he had enough data to see some pattern emerging in the crystallographic studies of the new compounds we now call actinides. Willy called this the Thoride Series, because everything was happening after thorium, and he did this *before* Glenn T. Seaborg proposed the Actinide Series. So, it may be that Willy discovered this correlation and series. Subsequently, Willy and Finley Ellinger, with hints from Frank Schnettler and others' work on physical properties, eked out the various crystal structures and later published them.[2,4–8] These papers, dating from 1950 to 1963, are remarkable. Many are short with few or no references. Some contain the entire paper's contents in the abstract. There were no computers when many of them were written. And there are only one or two authors on each paper. In terms of understanding plutonium and its electronic structure, these papers are revealing.

From basic thermodynamics, the plutonium crystal structure that exists near zero temperature is the only one not influenced by entropy and hence is controlled only by energy. For plutonium, the structure is completely bizarre, being monoclinic α phase with 16 atoms per unit cell, and having eight different distinct plutonium sites and some very short interatomic bonds. Zachariasen needed to reinvent some aspects of structure determination to solve this structure from the powder patterns because no single crystals could be produced.[9] With these new tools, he says, *"No novel principles are involved, no computational aids are required, and only the most elementary knowledge of lattice geometry is needed . . . one looks for recurrent values of differences."*[10]

For an elemental metal, how can a monoclinic structure be the answer? In fact, for plutonium one should really ask, how can it not? With seven 5*f* electronic orbitals, each with a complex radial and spatial electron density distribution, it seems that plutonium can lower its energy by making four very short bonds from these orbitals in a way that reasonable electronic structure calculations can capture. With increasing temperature, β-phase plutonium forms as body-centered monoclinic crystals,[4,8] now with

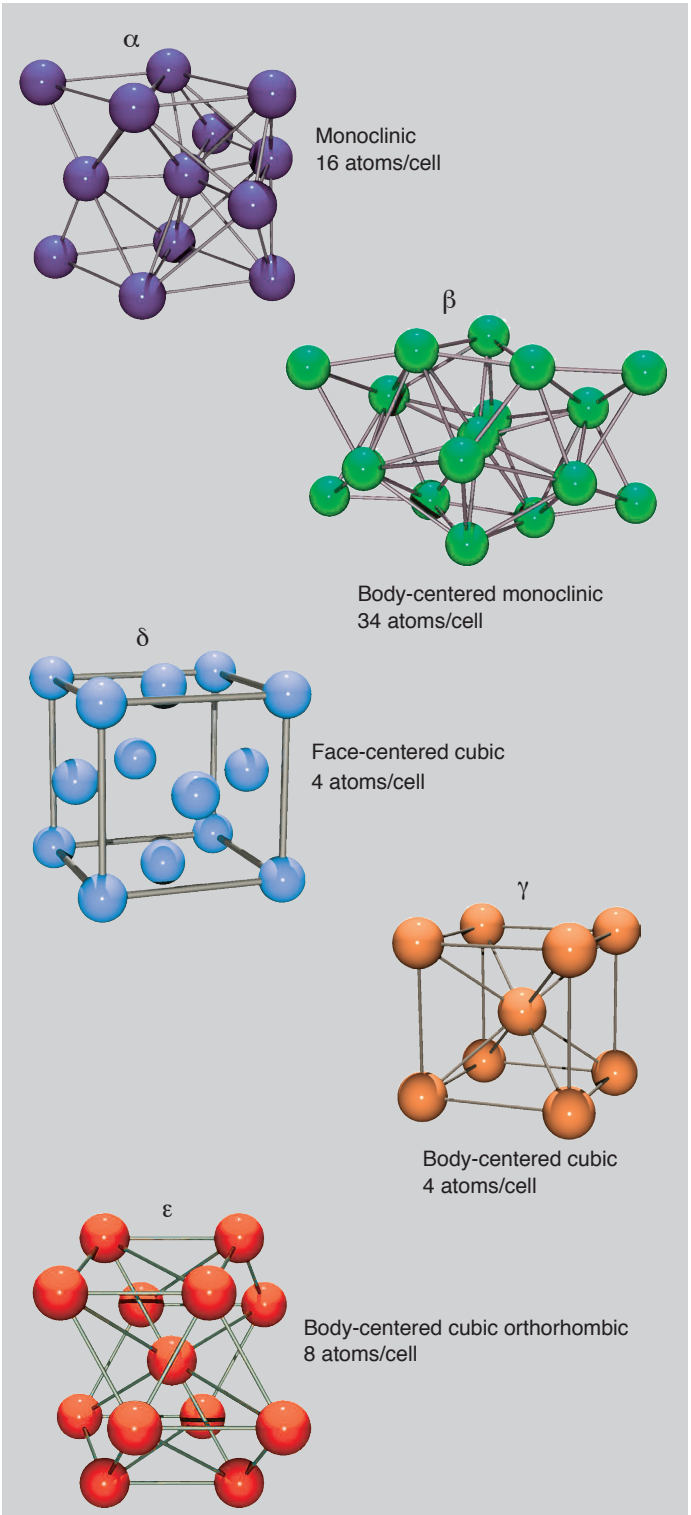

*While work at Los Alamos was still heavily classified, Frank Schnettler and his team reconfirmed that plutonium had **five** phases. Shown here are modern models of the five easily distinguished crystal structures of plutonium. δ-prime, omitted, looks just like ε.*

34 atoms per unit cell but "only" seven different sites. For both α and β phases, Zachariasen writes, *"All attempts to prepare single crystals of beta plutonium large enough for x-ray diffraction studies have failed. Accordingly, the structure determination had to be deduced entirely from 'powder' diffraction patterns."* And without a decent computer, too! *"The intensities were measured by planimetering the area under the diffraction peaks."*[4,12]

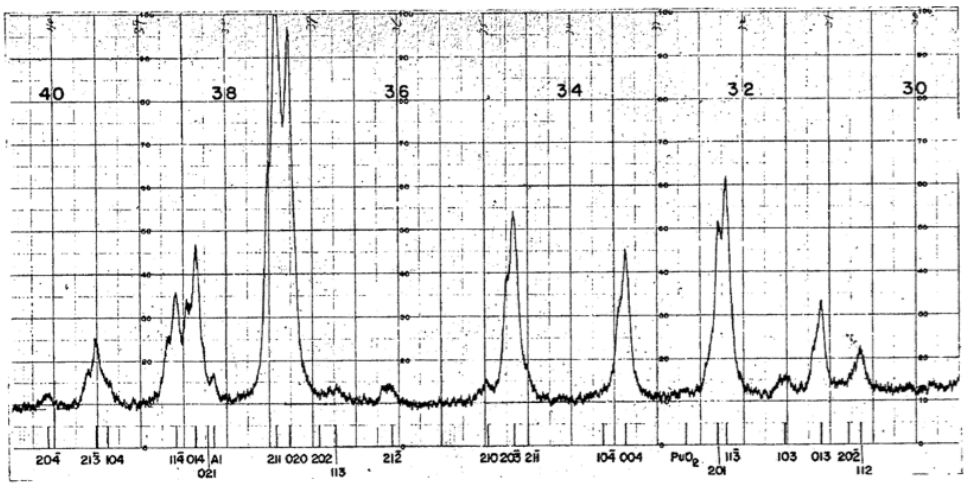

The raw x-ray reflections for α plutonium. Intensities were computed with a mechanical planimeter from graphs of this quality, as reported by Zachariasen et al., in "The Crystal Structure of Beta Plutonium Metal," in Acta Crystallographa *in 1963.*

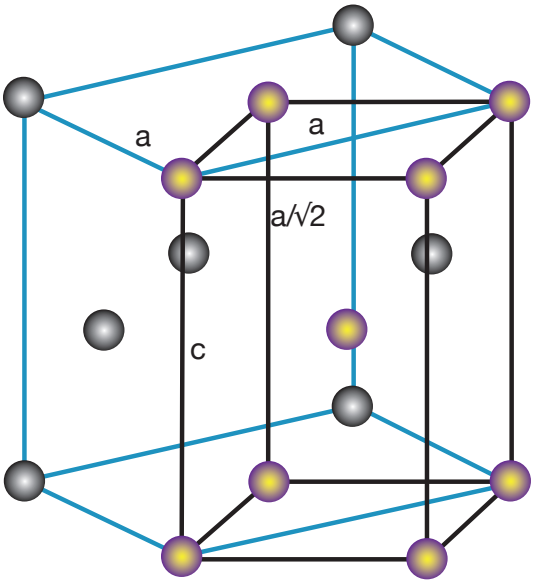

*Paths of tetragonal states between two phases of a material, such as bcc and fcc, are called Bain paths. In the above face-centered cubic and body-centered tetragonal representation, compression along **c** takes δ plutonium (blue-fcc) to ε plutonium (black-bcc) when the compression of **c/a** equals 2½. The plutonium system is very soft to such distortion.*

As plutonium is heated above the β phase, it becomes increasingly symmetric while remaining strange, advancing through a series of crystalline structures. These phases transition from the body-centered orthorhombic[5,12] γ phase, to the face-centered cubic δ phase with a negative coefficient of thermal expansion (a close-packed structure and the lowest density of any phase of plutonium[2]), and finally to the body-centered cubic[2] ε phase with higher density than the colder phase just below it. Here, we dismiss the δ-prime phase as unimportant because a simple distortion (compression along a cubic axis) of δ plutonium produces δ-prime plutonium and then ε plutonium when the distortion equals $2^{1/2}$. The latent heat is negligible, and the error bars of the x-ray determination of δ-prime are the highest by an order of magnitude than for any phase of plutonium.[2] Thus it is likely that the sluggishness of the δ-to-ε transition simply leaves a local strain field in which weakly distorted δ (which is what δ-prime looks like) remains until the transition is complete.

Jette describes some incredibly revealing gems about the phases above β. *"It is to be specially noted that for no phase do both the coefficient of thermal expansion and the temperature coefficient of resistivity have the conventional sign. Thus, if the phase expands on heating, the resistance decreases."* And, he further states,*"Perhaps the most striking feature of the crystal structure data is that the δ phase, which has the lowest density of any phase in the entire system, is the only phase with a close-packed structure. The increase in density in going from the face-centered cubic δ to the body-centered cubic ε is noteworthy."*[2]

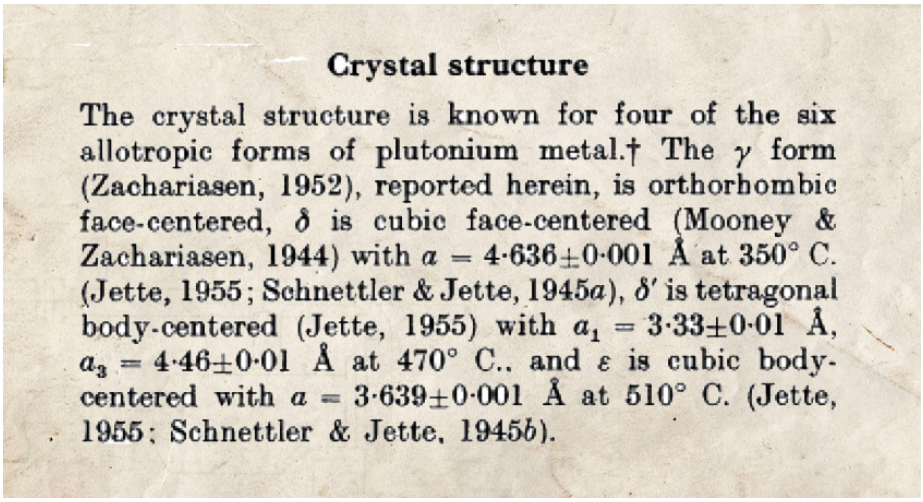

Crystal structure

The crystal structure is known for four of the six allotropic forms of plutonium metal.† The γ form (Zachariasen, 1952), reported herein, is orthorhombic face-centered, δ is cubic face-centered (Mooney & Zachariasen, 1944) with $a = 4{\cdot}636 \pm 0{\cdot}001$ Å at 350° C. (Jette, 1955; Schnettler & Jette, 1945*a*), δ' is tetragonal body-centered (Jette, 1955) with $a_1 = 3{\cdot}33 \pm 0{\cdot}01$ Å, $a_3 = 4{\cdot}46 \pm 0{\cdot}01$ Å at 470° C., and ε is cubic body-centered with $a = 3{\cdot}639 \pm 0{\cdot}001$ Å at 510° C. (Jette, 1955; Schnettler & Jette, 1945*b*).

Paragraph scanned from Zachariasen and Ellinger, "The Crystal Structure and Thermal Expansion of γ-Plutonium," 1955.[12] The error in the determination of the crystal structure of δ-prime plutonium is an order of magnitude greater than for any other phase.

The strangeness reaches a zenith with the work of Lawson et al.,[11] and Migliori et al.[13–16] Lawson et al., used modern methods to measure the lattice parameters of gallium-stabilized δ plutonium with gallium concentrations such that the thermal expansion coefficients range from positive to negative. Lawson and his collaborators were able to fit the measurements quite nicely using a two-component (invar) model.[11] Freibert and Migliori established that extrapolations of elastic moduli of delta plutonium containing gallium match the elastic moduli of δ plutonium without gallium at temperatures where both exist as δ plutonium.[17] However, Migliori also established that from about 350 K to 800 K (where Lawson found that the thermal expansion, depending on gallium concentration, of δ plutonium was positive, zero, or negative), the adiabatic bulk modulus dropped about 10% on warming, about an order of magnitude greater than what aluminum would do, and independent of the sign of the thermal expansion.[14–15]

This change in adiabatic bulk modulus on warming, combined with the strange resistivity results reported by Jette,[2] is outside the ability of any ab initio electronic structure model to capture. Here's why: Any electronic structure model using any form for electron orbitals places atoms in a crystal pattern, and then computes the total energy to find a minimum at some value of lattice parameter, based upon a very broad range of possible assumptions about potentials and orbitals. The adiabatic bulk modulus (the stiffness against hydrostatic compression) is determined by taking the final solution and simply computing the ratio of the change in energy to a change in volume (or lattice parameter), keeping all electron occupation numbers fixed, which is an easy thing to do. Temperature does not come into such a calculation. Thus we must ask, "How can the bulk modulus change by the same 10% when the volume increases, decreases, or does not change at all?"

The inescapable conclusion is that volume is unimportant in understanding δ plutonium, the most important metallic form for our mission, and that simply knowing the structures and stiffnesses raises deep fundamental-science questions about plutonium that may be at the cutting edge of correlated-electron physics. If we consider together the monoclinic phases,

"How can the bulk modulus of δ plutonium change by the same 10% when the volume increases, decreases, or does not change at all?"

"The inescapable conclusion is that volume is unimportant in understanding δ plutonium."

Acknowledgements

This work was supported as part of the Materials Science of Actinides, an Energy Frontier Research Center funded by the U.S. Department of Energy, Office of Science, Basic Energy Sciences, under Award #DE-SC0001089.

the strange effect of δ plutonium being in a close-packed structure but with the lowest density of any form of plutonium, and the odd behavior of the bulk modulus with temperature and volume changes, it is clear that very much more complex physics is required before we have even a minimal understanding of plutonium.

References

1. *Monthly Progress Report of the Chemistry and Metallurgy Division,* Report LAMS-211, Los Alamos Scientific Laboratory, Los Alamos, NM, 1945.
2. Jette, E. R., Some Physical Properties of Plutonium Metal. *Journal of Chemical Physics,* **1955**, *23*.
3. *Monthly Progress Report of the Chemistry and Metallurgy Division*, Report LAMS-249, Los Alamos Scientific Laboratory, Los Alamos, NM, 1945.
4. Zachariasen, W. H.; Ellinger, F. H. Unit Cell and Thermal Expansion of β Plutonium Metal. *Acta Crystallogr.* **1959**, *12(3)*, 175–176.
5. Zachariasen, William H. *The Crystal Structure of Gamma Plutonium,* Report LA-01325, Zachariasen, William H., U. S. Atomic Energy Commission, Ed. Los Alamos Scientific Laboratory, Los Alamos, NM,1951.
6. Zachariasen, W. H.; Finley, E. Crystal Structure of Alpha Plutonium Metal. *J. of Chem. Phys.* **1957**, *27*, 811.
7. Zachariasen, W. H.; Ellinger, F. H. The Crystal Structure of Alpha Plutonium Metal. *Acta Crystallogr.* **1963**, *16(8)*, 777–783.
8. Zachariasen, W. H.; Ellinger, F. H. The Crystal Structure of Beta Plutonium Metal. *Acta Crystallogr.* **1963**, *16(5)*, 369–375.
9. Zachariasen, W. H. A New Analytical Method for Solving Complex Crystal Structures. *Acta Crystallogr.* **1952**, *5(1)*, 68–73.
10. Zachariasen, W. H. Interpretation of Monoclinic Powder X-Ray Diffraction Patterns. **1963**, *16(8)*, 784–788.
11. Lawson, A. C., et al. Invar Model for Δ-Phase Pu: Thermal Expansion, Elastic and Magnetic Properties. *Philos. Mag.* **2006**, *86(17-18)*, 2713–2733.
12. Zachariasen, W. H.; Ellinger, F. H. Crystal Chemical Studies of the 5-*f* Series of Elements. XXIV. The Crystal Structure and Thermal Expansion of γ-Plutonium. *Acta Crystallogr.* **1955**, *8*, 431–433.
13. Migliori, A., et al., Unexpected Elastic Softening in Delta-Plutonium. *Phys. Rev. B.* **2006**, *73(5)*, 052101-1–4.
14. Migliori, A., et al., Alpha-Plutonium's Polycrystalline Elastic Moduli over Its Full Temperature Range. *J. Acoustical Soc.* **2007**, *122(4)*, 1994–2001.
15. Migliori, A., et al., Temperature Dependence of Elastic Moduli of Polycrystalline β-Plutonium. *Phys. Rev. B.* **2011**, *84*.
16. Stroe, I., et al., Polycrystalline Gamma-Plutonium's Elastic Moduli Versus Temperature. *J. Acoustical Soc.* **2010**, *127(2)*,741–745.
17. Freibert, F. J., et al., Elastic Moduli of Unalloyed Delta Plutonium, Putonium Futures the Science 2012 Conference Proceedings, Cambridge, UK, p. 42. July 2012.

$PuCoGa_5$:
A Plutonium-Based Superconductor

This article was contributed by John L. Sarrao, Theory, Simulation and Computation, and Eric D. Bauer, Condensed Matter and Magnet Science, both at Los Alamos National Laboratory.

For plutonium in its metallic solid state, the face-centered-cubic delta (δ) phase is arguably its most important crystal structure. In this article we make the case that the tetragonal $HoCoGa_5$ (or 115) crystal structure may be challenging the status of δ-Pu. Further, it is ironic and not accidental that the 115 structure is a layered derivative of δ-Pu. The structural similarities between the 115 structures and δ-Pu suggest that their physical properties are probably more related than apparent at first glance and that studies of one material may be useful in understanding the other.

At room temperature, pure plutonium exists in the monoclinic alpha (α) phase. Face-centered-cubic δ-Pu is stable at elevated temperatures. Whereas α-Pu behaves metallurgically like cast iron, δ-Pu has properties that are similar to aluminum, greatly facilitating machining and applications. Although the δ phase of pure plutonium is stable in only a limited temperature range, the addition of small amounts of various alloying agents, with gallium being among the most common, increases the range of stability of δ-Pu to include room temperature. Although important open questions remain about the evolution from α- to δ-Pu and the associated changes in physical properties, it is generally understood that the partial localization of the plutonium 5*f* electrons plays a key role. In α-Pu, the 5*f* electrons are delocalized and contribute to chemical bonding; in δ-Pu, the 5*f* electrons become partially localized, leading to a simpler crystal structure, an enhanced effective mass of the conduction electrons, and physical properties consistent with δ-Pu being nearly magnetic. This complex evolution of f-electron behavior leading to the stability of elemental plutonium in such a simple crystal structure is what makes face-centered-cubic δ-Pu the most important crystal structure for metallic solid-state plutonium.

Study of the connection between partially localized f-electron behavior and the properties of elemental plutonium has at least a 40-year history at Los Alamos. In the late 1970s and early 1980s, Los Alamos scientists Sig Hecker, Jim Smith, and Zach Fisk, among others, helped define a class of materials known as heavy fermions, with the name deriving from the enhanced electron effective mass that results from the hybridization of conduction electrons with partially localized f-electrons. These materials straddle the boundary between magnetic and superconducting behavior, and the first uranium-based heavy fermion superconductors were discovered at Los Alamos in the early 1980s. Through the 1980s and 1990s, Los Alamos was a principal driver in the international effort to understand the behavior of f-electron materials and the novel ground states that resulted in these compounds.

A renaissance and revolution in the field of heavy fermion superconductivity occurred in 2001 with the discovery of $CeRhIn_5$. $CeRhIn_5$ crystallizes in the tetragonal $HoCoGa_5$ structure and is a layered

Compounds whose elements are in a 1:1:5 ratio, such as $CrCoIn_5$, $PuCoGa_5$, and $HoCoGa_5$, are known as "one-one-five compounds" or "115 compounds" when they are described to emphasize their molecular structure.

An element's atomic number increases as its electron count increases, filling available energy states. These energy states are organized into shells, each of which is designated by an integer. Within each shell, each orbital is designated by a letter. Elements are grouped by shells and orbitals in the periodic table of elements. The actinide elements are those with the f *orbital of the fifth shell electronically occupied; i.e., the 5*f *elements.*

> *"The vast majority of these compounds either superconduct at low temperatures or can be made to do so with applied pressure."*

variant of $CeIn_3$, which occurs in the same face-centered-cubic structure as δ-Pu. $CeIn_3$ orders antiferromagnetically near 10 K, and when subjected to very high pressure becomes a superconductor at 200 mK. When layers of $CeIn_3$ are alternated with layers of $RhIn_2$, $CeRhIn_5$ results. This layering decreases the magnetic ordering temperature from 10 K to 3.8 K and upon application of pressure, increases the superconducting transition temperature from 250 mK to 2.1 K. This reduction of magnetic-ordering temperature and increase of superconducting transition temperature is consistent with theoretical expectations for superconductivity mediated by magnetic fluctuations. Following the discovery of $CeRhIn_5$ and its pressure-induced superconductivity, discovery of ambient pressure superconductivity in $CeIrIn_5$ and $CeCoIn_5$ quickly followed.

If one follows the analogy of alternating layers of $CeIn_3$ and MIn_2 (where M is a transition metal), one can imagine stoichiometries consistent with multiple layers of either $CeIn_3$ or MIn_2. In fact, Ce_2MIn_8 and CeM_2In_7 have been reported in recent years for a variety of transition metals such as cobalt, rhodium, iridium, palladium, and platinum. The crystal structures of these materials and their structural relationships are shown in the figure below. Furthermore, the vast majority of these compounds either superconduct at low temperatures under ambient conditions or can be made to do so with applied pressure. At present, the majority of all known heavy fermion superconductors crystallize in the $HoCoGa_5$ structure or its layered derivatives.

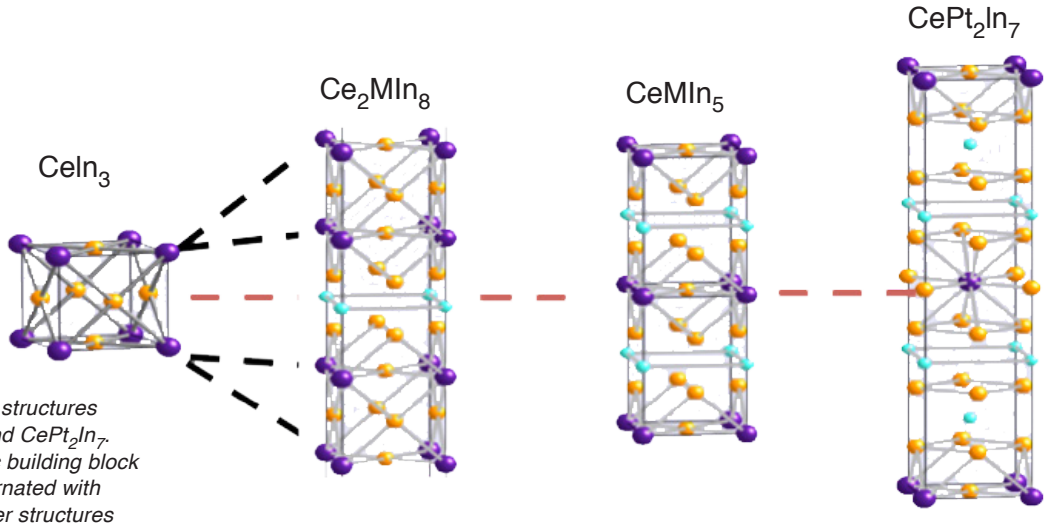

A representation of the crystal structures of $CeIn_3$, Ce_2MIn_8, $CeMIn_5$, and $CePt_2In_7$. The $CeIn_3$ unit forms the basic building block of the structure and when alternated with MIn_2 (1:1, 2:1, or 1:2), the other structures result. In the case of $PuCoGa_5$, the building blocks are $PuGa_3$ and $CoGa_2$. Although $PuGa_3$ is not stable at room temperature in this face-centered-cubic structure, it does correspond notionally to replacing three out of every four plutonium atoms in δ-Pu with gallium.

Given the historical association of δ-Pu and heavy fermion behavior, it was not long after the discovery of $CeRhIn_5$ that attempts were made to form plutonium intermetallic compounds in the 115 structure. While initial attempts to make, for example, $PuCoIn_5$, were unsuccessful, replacing indium with gallium led to more fruitful results. $PuCoGa_5$ was discovered in 2002 as the first plutonium-based superconductor, crystallizing in the same $HoCoGa_5$ structure as its cerium-based counterparts. The superconducting transition temperature (Tc) of $PuCoGa_5$ is a remarkable 18.5 K, nearly a factor of ten higher than that for other known heavy fermion superconductors.

With this discovery, the early work of Hecker, Smith, and Fisk came full circle. By creating a layered variant of δ-Pu, a record-high superconducting transition temperature for heavy fermion superconductors was established. Further experiments have shown that the properties of $PuCoGa_5$ are consistent with partially localized f-electron behavior. The nature of the superconductivity is still unknown, although it is clear that it is unconventional and not mediated by phonons, as is found in simple metals. The wealth of data indicates that the unconventional superconductivity in the cerium-based 115 materials is mediated by antiferromagnetic spin fluctuations. These antiferromagnetic spin fluctuations may also be present in the plutonium 115 materials, but charge (valence) fluctuations are also a possible source of the superconductivity.

As in the case of cerium-based 115 materials, the $HoCoGa_5$ structure has been fertile ground for the discovery of additional plutonium superconductors. In fact, all known plutonium superconductors, $PuCoGa_5$ (Tc = 18.5 K), $PuRhGa_5$ (Tc = 8.7 K), $PuCoIn_5$ (Tc = 2.5 K), and $PuRhIn_5$ (Tc = 1.7 K), are members of the 115 family. As the images in the three crystal photographs shown below indicate, it is possible to grow relatively large single crystals of these compounds, and their exploration through a variety of measurement techniques is currently underway. The physics of these 115 materials is similar to that of δ-Pu. An analogy between the effects of applied physical pressure and chemical pressure (which results because, for example, gallium and indium have different ionic radii) explains a number of the novel phenomena that have been observed.

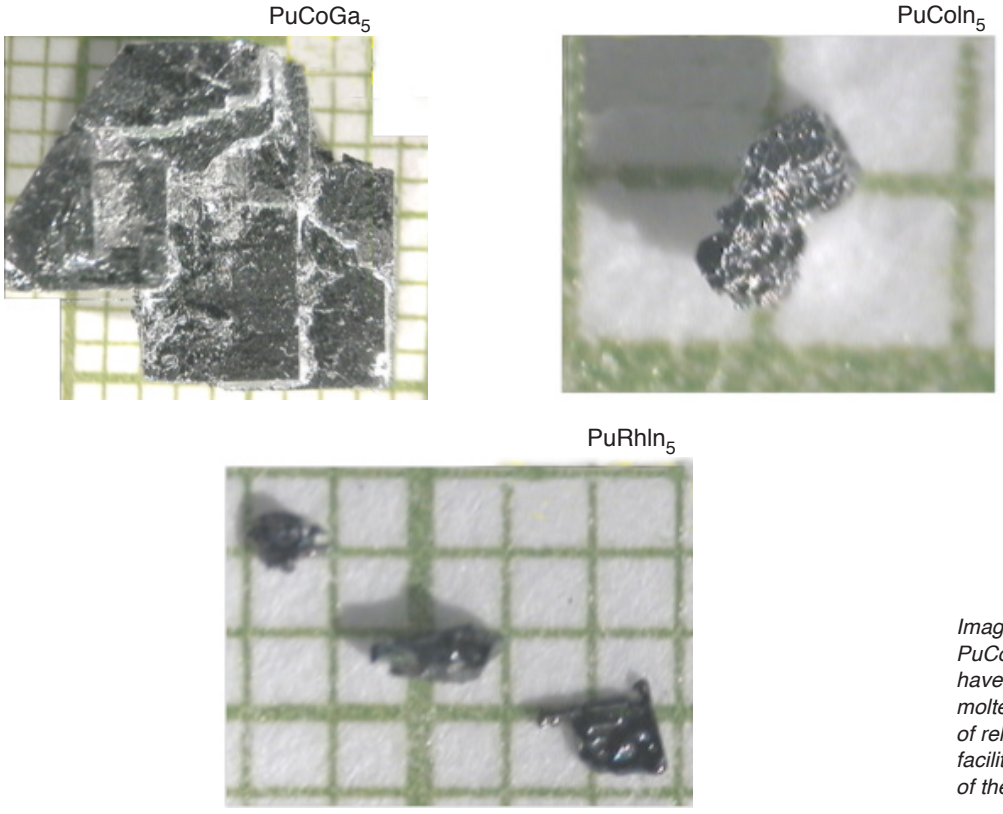

Images of single crystals of $PuCoGa_5$, $PuCoIn_5$, and $PuRhIn_5$. These materials have all been grown at Los Alamos using molten metal flux techniques. The existence of relatively large single crystals greatly facilitates the study of the physical properties of these face-centered-cubic 115 materials.

Acknowledgments

The physical infrastructure and intellectual environment that exists at Los Alamos National Laboratory because of our mission responsibility to steward plutonium was a key enabler for this work. We acknowledge our many colleagues and collaborators in the actinide science community at Los Alamos and thank them for their support.

One of the exciting consequences of discovering such a large number of isostructural materials is that trends can be extracted. As was discussed above, the bi-layer variants of 218 and 127 materials provide insights into 115 materials. In the case of $PuCoGa_5$ (as well as $CeMIn_5$), it is interesting that not only are $PuCoGa_5$ and $PuRhGa_5$ stoichiometric superconductors, but the intermediate alloy Pu(Co or Rh)Ga_5 also superconducts. When one examines these data, the trend that emerges is that Tc has a linear relationship to the ratio of the tetragonal lattice constant (c/a) independent of chemical composition, as shown in the plot of c/a values. The conclusion that one draws is that the spacing between alternating layers of $PuGa_3$ and $CoGa_2$ is directly correlated with superconducting transition temperature in a way that is unlike any other independent structural parameter.

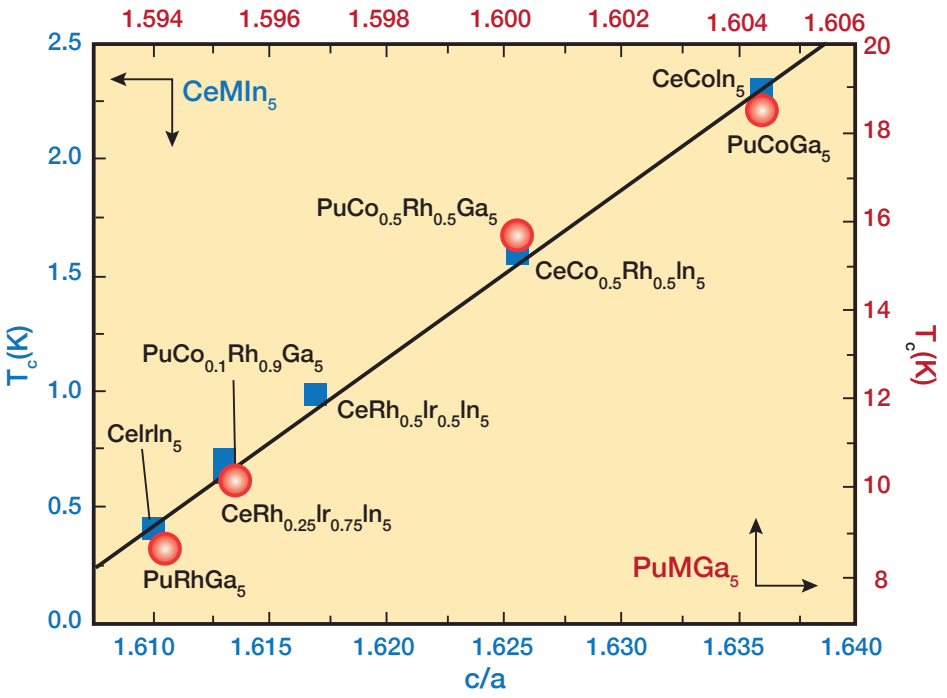

The superconducting transition temperature, Tc, for a variety of Ce-based (blue squares) and Pu-based (red spheres) 115 materials is plotted against the ratio of the tetragonal lattice constants, c/a. The strong correlation between Tc and c/a reveals the important role of the tetragonal crystal structure in producing high transition temperatures that are somewhat independent of chemical composition.

This brief survey of work over the last decade suggests that the $HoCoGa_5$ structure both revolutionized heavy fermion superconductivity in general and launched the new field of plutonium superconductivity. In just the case of plutonium 115 materials, more than 100 papers have been published since 2002. The partially localized electron behavior that characterizes δ-Pu is the essential physics that many subsequently published papers explore.

We have made a compelling argument that the tetragonal $HoCoGa_5$ structure might be displacing face-centered-cubic δ-Pu as the most interesting crystal structure for plutonium in its metallic solid state. However, our best hope is that the 115 structure is replaced by another new and more interesting crystal structure, because that would signal the emergence of an even more fertile set of materials for understanding the condensed matter physics of elemental plutonium.

Structural Determination of the First Molecular Plutonium–Tellurium Bond: f-Element Soft Donor Bonding Studies

The Pu(III)[N(TeP^{i}Pr$_2$)$_2$]$_3$ Complex

This article was contributed by Andrew J. Gaunt, Inorganic, Isotope, and Actinide Group, Chemistry Division, Los Alamos National Laboratory.

The Scientific Challenge

If nuclear fission is to continue to contribute significantly to the U.S. energy portfolio, issues surrounding processing and disposition of used nuclear fuel need to be addressed.[1,2] A component of many advanced nuclear fuel cycle options includes novel actinide separations technologies that would facilitate strategies aimed at reducing the radiotoxic lifetime and volume of radioactive waste that requires burial at a geological repository site. As an example of one proposed option, certain actinide (An) isotopes with long half-lives that are present in the used fuel would be recycled into new fuel and "burned up" or "consumed" in the reactor.[3] This process of actinide transmutation could only occur after the lanthanide (Ln) fission products also present in the used nuclear fuel are separated because they would otherwise act as neutron poisons and impede the transmutation process. This is a very difficult separation to achieve because of the similar chemical behavior of trivalent An(III) and Ln(III) ions, both of which are considered to be "hard" Lewis acidic metal cations that engage in predominately ionic bonding. Hard donor ligands, such as those bearing oxygen donor atoms, tend to bind strongly to both An(III) and Ln(III) ions but are unable to discriminate one set of ions from the other. However, certain "soft" donor ligands (such as nitrogen and sulfur atom donors) display selectivity for An(III) in preference to Ln(III), a phenomenon believed to arise as a result of slightly greater covalent bonding in the An–ligand than in the Ln–ligand interaction.[4] The scientific challenge is that covalent interactions and electronic structure details in actinide soft donor chemistry are poorly understood, with little supporting experimental evidence for covalency as a conclusive explanation for the behavior of actinide selective extraction agents.

The chemistry of the transuranic elements (those sitting to the right of uranium in the 5*f* series of the periodic table) provides an underpinning chemical science basis to develop novel separation and waste processes, such as the trivalent actinide and lanthanide example given in the foregoing paragraph. Although extensive research focus has been placed on the less-radioactive early actinide elements of uranium and thorium,[5] the chemistry of neptunium, plutonium, americium, and curium is far less studied despite the fact that these transuranic elements are often far more problematic because of chemical control and hazardous waste considerations. One of the reasons for this research disconnect is that chemical manipulations of the transuranic elements usually require specialized radiological facilities and safety infrastructure, such as those found at Los Alamos National Laboratory.

"Hard donor ligands bearing oxygen donor atoms tend to bind strongly to both actinide(III) and lanthanide(III) ions. Soft donor ligands bearing nitrogen or sulfur display selectivity for actinides in preference to lanthanides."

Although there are a few exceptions, transuranic chemical research at universities is rarely encountered. In contrast, uranium and thorium (primarily as the weakly radioactive ^{238}U and ^{232}Th isotopes) chemistry can be routinely studied at many universities.

To gain a detailed understanding of chemical bonding at a level that can be used to predict and control actinide behavior in separations, it is important to define bonding trends across all the relevant actinide elements. To work toward this goal, we undertook a study of soft donor bonding with both U(III) and Pu(III) actinide ions in comparison with La(III) and Ce(III) ions, respectively, and uncovered bond-length differences using x-ray crystallography as an experimental indicator of covalency differences. This work included the first structurally characterized U-Te and Pu-Te molecular bonds, which were rare examples of hard-metal–soft-ligand interactions in lanthanide or actinide complexes. The discovery of these bond length differences was particularly significant for the plutonium complex because of the general lack of molecular structural determinations of molecular complexes for plutonium.

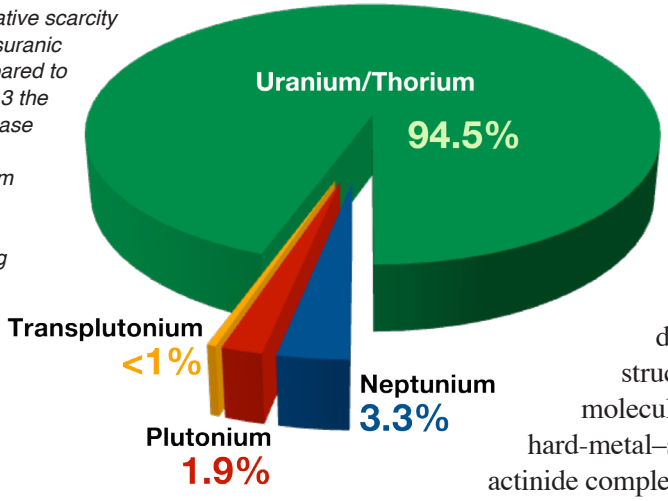

This pie chart shows the relative scarcity of known structures for transuranic molecular compounds compared to uranium and thorium. In 2013 the Cambridge Structural Database had on deposit 4102 crystal structures containing uranium or thorium, 140 containing neptunium, 81 containing plutonium, and 18 containing transplutonium actinides.

What We Learned

The imidodiphosphino–chalcogenide ligand class was identified as an ideal system for making systematic comparisons of An(III) and Ln(III) bonding across a range of soft donor complexes. First, imidodiphosphino–chalcogenide ligands facilitate the formation and isolation of homoleptic complexes (having only one type of ligand in the metal inner coordination sphere), which provides more cogent comparisons between bonds of interest because potential interference from secondary ligands has been eliminated. Second, the identity of the soft donor atom can be interchanged between sulfur, selenium, and tellurium within a series of otherwise identical molecules, enabling variation of different donor atom electronegativities (or degree of "softness"). Third, the steric bulk of the ligand (i.e., how much space the ligand occupies) can be changed by installation of different-size components on the ligand framework (specific to this research, either phenyl rings or the more sterically demanding iso-propyl groups were investigated). Fourth, the ligand framework forms stable complexes with both U(III) and Pu(III), thereby making it possible to investigate the effect of different actinide metal electropositivities (in contrast, many other ligand frameworks can lead to oxidation of U(III) to U(IV) complexes). For comparisons to lanthanides, we chose La(III) and Ce(III) to compare with U(III) and Pu(III), respectively, because each pair has near identical ionic radii,[6] meaning that any significant bond length differences between isostructural complexes is unlikely to be attributable to differences in ionic bonding.

Syntheses of both lanthanide and actinide complexes were accomplished by reaction of the protonated imidodiphosphinochalcogenide ligand, $NH(EPR_2)_2$ (where E = S, Se; R = Ph, ^{i}Pr), with metal bis(trimethyl)-silylamide, $M[N(SiMe_3)_2]_3$ (where M = An, Ln), precursors leading to ligand deprotonation and formation of 1:3 metal to soft donor complexes, as shown in Scheme 1. In the case where R = ^{i}Pr and E = Te, an alternative synthetic strategy was employed using salt metathesis of lanthanide and actinide halide salts with a sodium salt of the soft donor ligand to result in formation of a 1:3 complex, as shown in Scheme 2. The alternative strategy was necessary because the P = Te bonds are relatively unstable compared with P = S and P = Se bonds, and the tellurium donor version of the ligand can only be isolated as a sodium salt and when stabilizing electron donating ^{i}Pr groups (instead of Ph rings) are present in the framework.

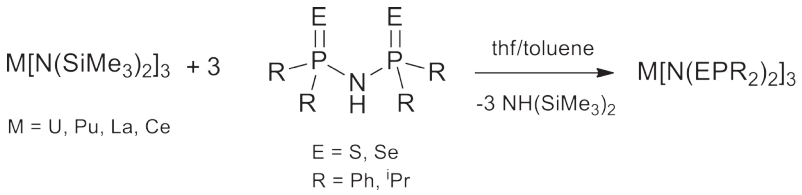

Scheme 1. The synthetic pathway in the preparation of the sulfur and selenium donor $M[N(EPR_2)_2]_3$ complexes.

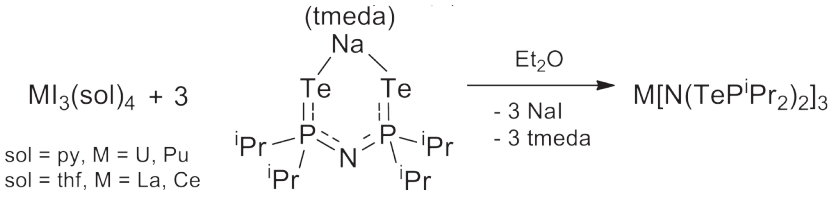

Scheme 2. Synthetic pathway in the preparation of the tellurium donor $M[N(TeP^iPr_2)_2]_3$ complexes. The sodium salt of the ligand is stabilized by the presence of tetramethylethylenediamine (tmeda). In the starting materials, sol is a solvent where py = pyridine, thf = tetrahydrofuran, and Et_2O = diethyl ether.

The crystal structures for the neutral $M[N(EPPh_2)_2]_3$ complexes (where E = S or Se) reveal homoleptic systems in which the imidodiphosphino-chalcogenide mono-anionic ligands coordinate in a tridentate fashion to the lanthanum, cerium, uranium, and plutonium metal centers. There are metal–ligand bonds to both of the chalcogen donor atoms as well as the nitrogen atom, with the coordination geometry around the metal center best described as distorted tricapped trigonal prismatic. The salient bond distances for comparison of An and Ln are presented in Table 1. A consistent pattern of shorter An–E versus Ln–E distance when comparing uranium to lanthanum and plutonium to cerium bonds is observed. The differences are statistically significant and greater than any differences that could be accounted for by the very small differences in the ionic radii of the An(III) and Ln(III) pairs being compared with each other. Therefore, the data support an assessment of a modest enhancement of covalency in the actinide–soft donor bonding compared with lanthanide–soft donor bonding. The same trend was observed in the $M[N(EP^iPr_2)_2]_3$ (where E = S, Se, Te) series of complexes (Table 2), in which the ligands are only bidentate through the two chalcogen donor atoms, thus removing any potential interference from the nitrogen donor atom.

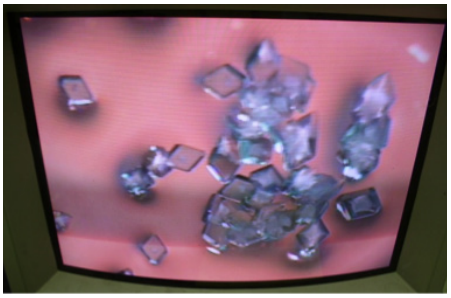

Photograph of x-ray diffraction quality single crystals of the $Pu[(SePPh_2)_2]_3$ complex with the imidodiphosphinochalcogenide mono-anionic ligands coordinated in tridentate fashion to the plutonium atoms.

Table 1. Selected Bond Distances for $M[N(EPPh_2)_2]_3$ Complexes

Compound	Bond	Distance, Å	Difference, Å
$U[N(SPPh_2)_2]_3$	U–S	2.9956	–
$La[N(SPPh_2)_2]_3$	La–S	3.0214	0.026
$Pu[N(SPPh_2)_2]_3$	Pu–S	2.9782	–
$Ce[N(SPPh_2)_2]_3$	Ce–S	3.0052	0.0270
$U[N(SePPh_2)_2]_3$	U–Se	3.0869	–
$La[N(SePPh_2)_2]_3$	La–Se	3.1229	0.0360
$Pu[N(SePPh_2)_2]_3$	Pu–Se	3.0710	–
$Ce[N(SePPh_2)_2]_3$	Ce–Se	3.1013	0.0303

In the six coordinate molecules in the $M[N(EP^iPr_2)_2]_3$ series, the geometry about the metal center is best described as distorted trigonal prismatic. Bond distance comparisons again span sulfur to selenium, but the R = ^{i}Pr group in the imidodiphosphinochalcogenide framework also enables access to tellurium as the soft donor atom because the P = Te bond is stabilized by the electron donating effect of the ^{i}Pr groups (in contrast, the P = Te bond is too unstable to permit isolation where R = Ph). The magnitude of the shortening of the An–E bond lengths compared to the Ln–E bond lengths is slightly greater than in the tridentate $M[N(EPPh_2)_2]_3$ complexes that also contain N–donor bonding and a higher metal coordination number of eight.

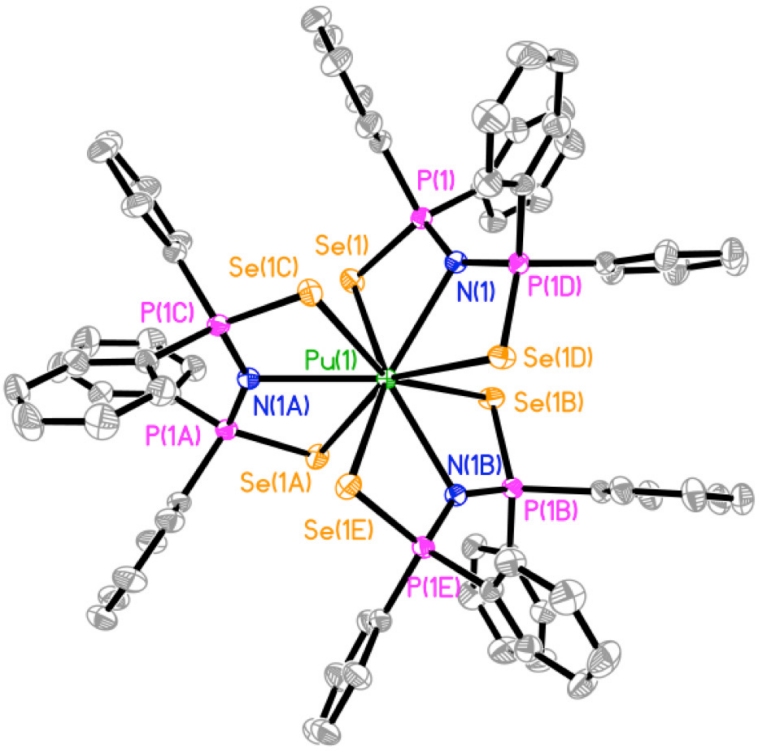

Thermal ellipsoid representation of the crystal structure the $Pu[(SePPh_2)_2]_3$ complex. All of the tridentate complexes where E = S, Se and M = La, Ce, U, Pu have identical molecular connectivity.

Table 2. Selected Distances for $M[N(EP^iPr_2)_2]_3$ Complexes

Compound	Bond	Average Distance, Å	Difference, Å
$U[N(SP^iPr_2)_2]_3$ $La[N(SP^iPr_2)_2]_3$	U–S La–S	2.854 2.892	– 0.038
$Pu[N(SP^iPr_2)_2]_3$ $Ce[N(SP^iPr_2)_2]_3$	Pu–S Ce–S	2.819 2.864	– 0.045
$U[N(SeP^iPr_2)_2]_3$ $La[N(SeP^iPr_2)_2]_3$	U–Se La–Se	2.964 3.019	– 0.055
$Pu[N(SP^iPr_2)_2]_3$	Pu–Se	2.917	–
$U[N(TeP^iPr_2)_2]_3$ $La[N(TeP^iPr_2)_2]_3$	U–Te La–Te	3.164 3.224	– 0.060
$Pu[N(TeP^iPr_2)_2]_3$ $Ce[N(TeP^iPr_2)_2]_3$	Pu–Te Ce–Te	3.123 3.182	– 0.059

A more simplistic way to think of this is that the "covalency differences" are spread over fewer bonds in the $M[N(EP^iPr_2)_2]_3$ complexes, resulting in a greater observable An versus Ln difference. Another trend also observable in the $M[N(EP^iPr_2)_2]_3$ complexes is that the magnitude of the An–E versus Ln–E distances increases as the electronegativity of the donor atom decreases from sulfur to selenium to tellurium (i.e., as the donor becomes "softer").

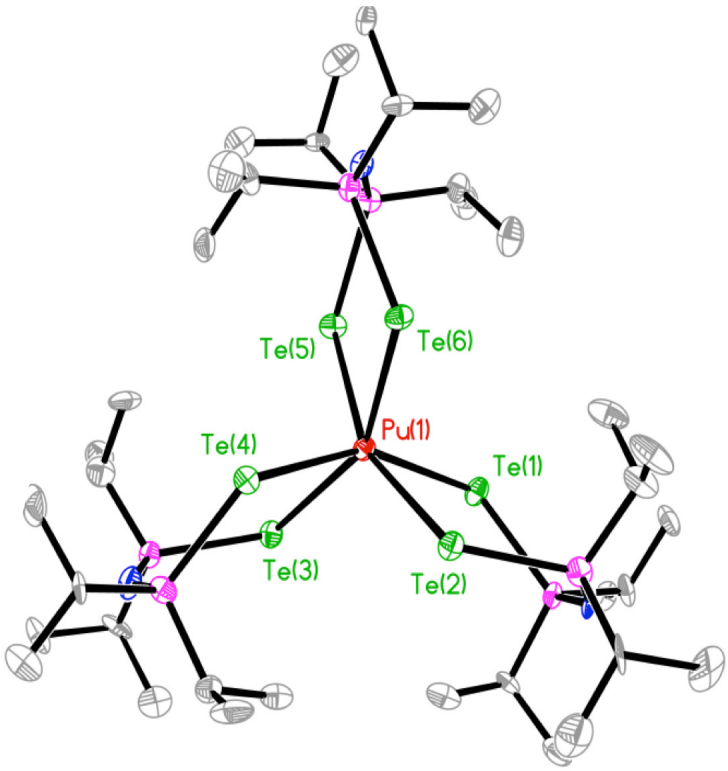

Thermal ellipsoid representation of the crystal structure of the $Pu[(TeP^iPr_2)_2]_3$ complex. All of the bidentate complexes, where E = S, Se, or Te and M = La, Ce, U, or Pu, have identical molecular connectivity. The exceptions are for M = Ce and E = Se, for which x-ray diffraction quality single crystals were not obtained, and therefore the structure could not be verified.

Acknowledgments

The work reported in this article was performed in the 2003–2008 timeframe under Department of Energy, Office of Basic Energy Sciences, Chemical Sciences Division, Heavy Element Chemistry Program funding. Andrew Gaunt was a postdoctoral researcher (as a Glenn T. Seaborg Fellow) at Los Alamos National Laboratory working with his mentor Mary Neu in the Chemistry Division. The density functional theory calculations were performed by Professor Nikolas Kaltsoyannis at University College London in the U.K. Andrew Gaunt is now a staff member in the Chemistry Division at Los Alamos National Laboratory and is currently supported by a Department of Energy, Office of Science, Early Career Research Program funding award, under which the more recent diselenophosphinate work has been conducted.

Conclusion

The conclusion from all of the metrical data is that, by carefully designing a systematic study, x-ray crystallography has proven to be an essential tool for uncovering indicators of covalency differences in f-metal soft donor systems that are relevant to actinide separation problems in the nuclear fuel cycle. The repeated observation of actinide bond shortening is consistent with the hypothesis that greater covalency is possible when employing soft donor ligands to preferentially bind An(III) ions over Ln(III) ions. This was the first study that could provide experimental support for this hypothesis in a systematic way by employing a range of soft donor atoms and showing that the bond shortening holds across two different elements in the 5*f* actinide series.[7] Density functional theory (DFT) calculations (performed by Professor Nikolas Kaltsoyannis at University College London in the U.K.) on model complexes agreed with the analysis of the experimental data. Enhanced covalency was found in the M–E bond as the chalcogen group is descended (sulfur to selenium to tellurium), mostly because of increased metal d-orbital participation. Conversely, although the overall f-orbital participation is smaller than that of the d-orbitals, it is an increase in the 5*f* versus 4*f* orbital participation that is responsible for the enhancement of covalency in the An–E versus Ln–E bonds.[7,8]

The Future

More recent studies have successfully extended these types of structural comparison studies to soft donor ligand systems, such as diselenophosphinates, that more closely resemble actinide extractant frameworks.[9] In collaboration with Los Alamos colleagues Stosh Kozimor and Enrique Batista, we are currently attempting to experimentally probe the electronic structure and bonding in these systems in more detail by applying the technique of ligand K-edge x-ray absorption spectroscopy and plan to extend the actinide work even further across the 5*f* series to encompass Am(III) chemistry.

References

1. Spent Fuel Processing Options, IAEA-TECDOC-1587, August 2008.
2. Basic Research Needs for Advanced Nuclear Energy Systems, Report of Basic Energy Sciences Workshop on Basic Research Needs for Advanced Nuclear Energy Systems, July 31-August 3, 2006.
3. Wigeland, R .A.; Bauer, T. H.; Fanning, T. H.; Morris, E .E. Repository Impact LWR MOX and Fast Reactor Recycling Options. *Nucl. Tech.* **2006**, *154*, 95.
4. See, for example, and references therein: (a) Jensen, M. P.; Bond, A. H. *J. Am. Chem. Soc.* **2002**, *124*, 9870. (b) Choppin, G. R. *J. Alloys Compd.* **2002**, *344*, 55. (c) Klaehn, J. R.; Peterman, D. R.; Harrup, M. K.; Tillotson, R. D.; Luther, T. A.; Law, J. D.; Daniels, L. M. *Inorg. Chim. Acta* **2008**, *361*, 2522.
5. Jones, M. B.; Gaunt, A. J. Recent Developments in Synthesis and Structural Chemistry of Nonaqueous Actinide Complexes. *Chem. Rev.* **2013**, *113*, 1137.
6. *Shannon, R. D. Acta Crystallogr.* ***1976****, A32,* 751.
7. Gaunt, A. J.; Reilly, S. D.; Enriquez, A. E.; Scott, B. L.; Ibers, J. A.; Sekar, P.; Ingram, K. I. M.; Kaltoyannis, N.; Neu, M. P. Experimental Theoretical Comparison of Actinide and Lanthanide Bonding in $M[N(EPR_2)_2]_3$ Complexes. *Inorg. Chem.* **2008***, 47*, 29.
8. Ingram, K. I. M.; Tassell, M. J.; Kaltsoyannis, N. *Inorg. Chem.* **2008**, *47*, 7824.
9. Jones, M. B.; Gaunt, A. J.; Gordon; J. C.; Kaltsoyannis, N.; Neu, M. P.; Scott, B. L., Uncovering f-Element Bonding Differences and Electronic Structure in a Series of 1:3 and 1:4 Complexes with a Diselenophospinate Ligand. *Chem. Sci.* **2013**, *4*, 1189.

Plutonium–Siderophore Single-Crystal Structure Launches Transuranic Biogeochemistry at Los Alamos National Laboratory

This article was contributed by Mary P. Neu, Strategic Improvement Office; John H. Matonic, Actinide Analytical Chemistry, Chemistry Division; Christy E. Ruggiero, Systems Design and Analysis, Nuclear Engineering and Nonproliferation Division; and Hakim Boukhalfa, Earth System Observations Group, Earth and Environmental Science Division; all at Los Alamos National Laboratory.

Introduction

In the mid to late 1990s, there was a resurgence of molecular transuranic chemistry at Los Alamos National Laboratory. At the same time, there was great and growing international interest in the environmental migration of early actinides (uranium, neptunium, plutonium, americium) from contaminated sites and an increasing desire to develop the technical basis for isolating nuclear waste in geologic repositories. In this context, we initiated research projects on the chemistry of actinides interacting with biological and environmental ligands: hydroxides, halides, nitrates, carbonates, peroxides, organic acids, aminocarboxylates, hydroxamates, siderophores, microbiological polymers, and humic acids.

One of our studies revealed the first structure of plutonium complexed by a biomolecule. That single-crystal structure of a plutonium–desferrioxamine siderophore compound inspired new hypotheses on how plutonium might interact with environmental bacteria, and launched transuranic biogeochemistry research at Los Alamos.

Plutonium–Siderophore Structure and Chemistry

The behavior of plutonium(IV) in aqueous solution is often described in relation to the well-understood processes for iron(III) because of their chemical similiarities. To predict the bioinorganic chemistry of plutonium, for example, we extrapolated from the chemistry that is known for iron.

Iron is an essential element for almost all organisms, from bacteria to mammals. Because iron exists naturally in many insoluble minerals, organisms have developed ways to solubilize, sequester, and take up, then store the nutrient iron that they require. A classic system involves siderophores (from the Greek: "iron carriers"), which are low-molecular-weight organic ligands that plants and microbes excrete to chelate iron and transport it across the cell membrane of the originating or other organisms. Based on this science, we proposed that plutonium would be solubilized by siderophores and stabilized as a Pu(IV) chelate complex. We tested this hypothesis using common ferrioxamine siderophores. When these siderophores were combined with several different starting forms of plutonium, ranging from soluble unchelated Pu(III, V, or VI), Pu(IV)EDTA, to low-solubility Pu(IV) hydroxide, to even insoluble fired Pu(IV) oxide, a soluble Pu(IV)–siderophore complex was formed. Once we confirmed that many chemical forms of plutonium could be chemically transformed

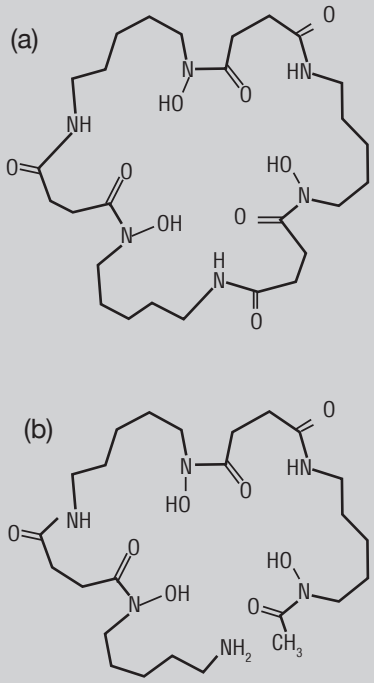

Desferrioxamine siderophores are produced in nature by soil bacteria. These siderophores are made up of hydroxamate groups that chemically bond metal ions, including Fe(III) and Pu(IV). In (a) the cyclic trihydroxamate is desferrioxamine E (DFE). In (b) the linear trihydroxamate is desferrioxamine B (DFB).

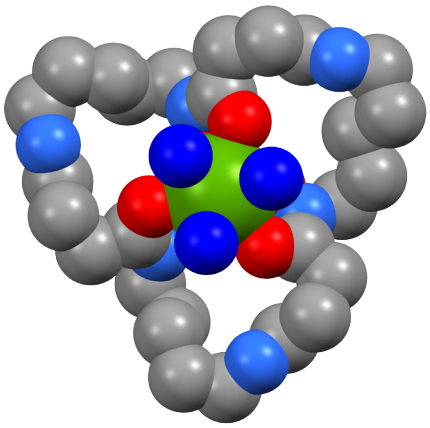

Shown here is the $[Pu(DFE)(H_20)_3]^+$ ion within the single-crystal structure of $[Al(H_20)_6]$ $[Pu(DFE)(H_20)_3]_2(CF_3SO_3)_5 \cdot 14H_20$ as reported by our team in the Angewante Chemie *International Edition in 2000.*

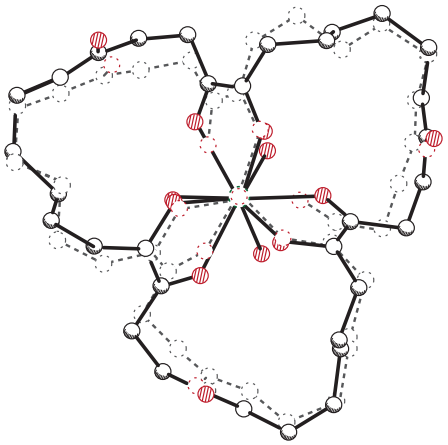

Overlaid structures of DFE complexes of Fe(III) and Pu(IV) show the same conformation of the ligand and ligand functional groups in the same orientation. The Fe(III)–DFE structure was published by the research group of D. van der Helm in the Journal of the American Chemical Society *in 1976.*

to a specific compound in water, we wanted to learn the structure of the compound and what that structure might suggest about how plutonium would interact with bacteria that use siderophores.

X-ray diffraction on crystals of Pu(IV)–DFE revealed a structure with some unexpected features, as shown in the accompanying figures. The Pu(IV) atom in the complex has bonds with nine oxygen atoms, six from the desferrioxamine on roughly one-half of the central plutonium, and three from water molecules on the other side of the plutonium. This structure was surprising because comparable structures of Th(IV) and Pu(IV) show the central metal atom is bound by eight more equally-spaced oxygens encircling the metal. The structure also has interesting similarities with and differences from the iron–siderophore structure. The overall shape and orientation of the DFE ligand is the same in the Pu(IV)–DFE and Fe(III)–DFE structures. The desferrioxamine has the flexibility to twist approximately 20 degrees to accommodate the different coordination geometry at the iron (octahedral, six Fe–O bonds) and plutonium (tricapped-trigonal prism, nine Pu–O bonds) centers. However, iron is completely encapsulated by the desferrioxamine ligand, whereas the larger plutonium has sites open to form bonds with water molecules.

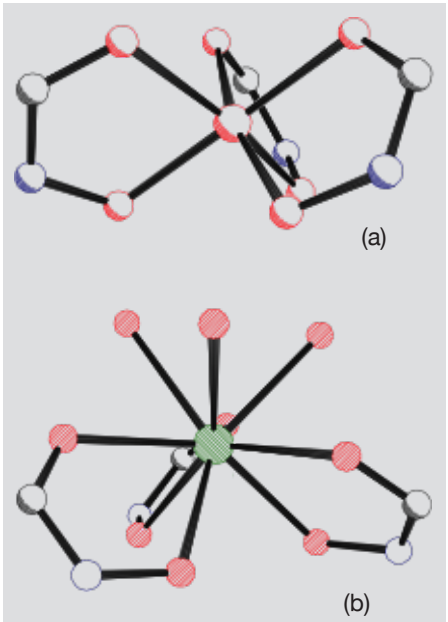

Coordination spheres of the Fe(III) and Pu(IV) metal ions in DFE structures. The iron ion in the DFE structure (a) is encapsulated in the siderophore molecule, whereas the larger plutonium ion (b) is not so encapsulated.

Impact on Plutonium Chemistry and Biogeochemistry

The structure of the Pu(IV)–DFE complex shows that in addition to the hydroxamate siderophore ligand, multiple water molecules are bound to the plutonium. This suggested to us that unlike Fe(III), Pu(IV) can form complexes where the plutonium is complexed by ligands in addition to the hexadentate siderophore, e.g., two siderophores, or a siderophore and a carbonate molecule, or a siderophore and one or more hydroxides, or even a siderophore and a mineral or bacterial surface. These possibilities strongly limit our ability to predict the plutonium species that can form and migrate in the environment. In further research, we and others confirmed that these species do form. Thus, these species can be included in computation models that are being used to certify international nuclear waste repositories, because we determined their thermodynamic stability constants. For example, in 2007

Mechanism Studies of Actinide-Microbe Interactions

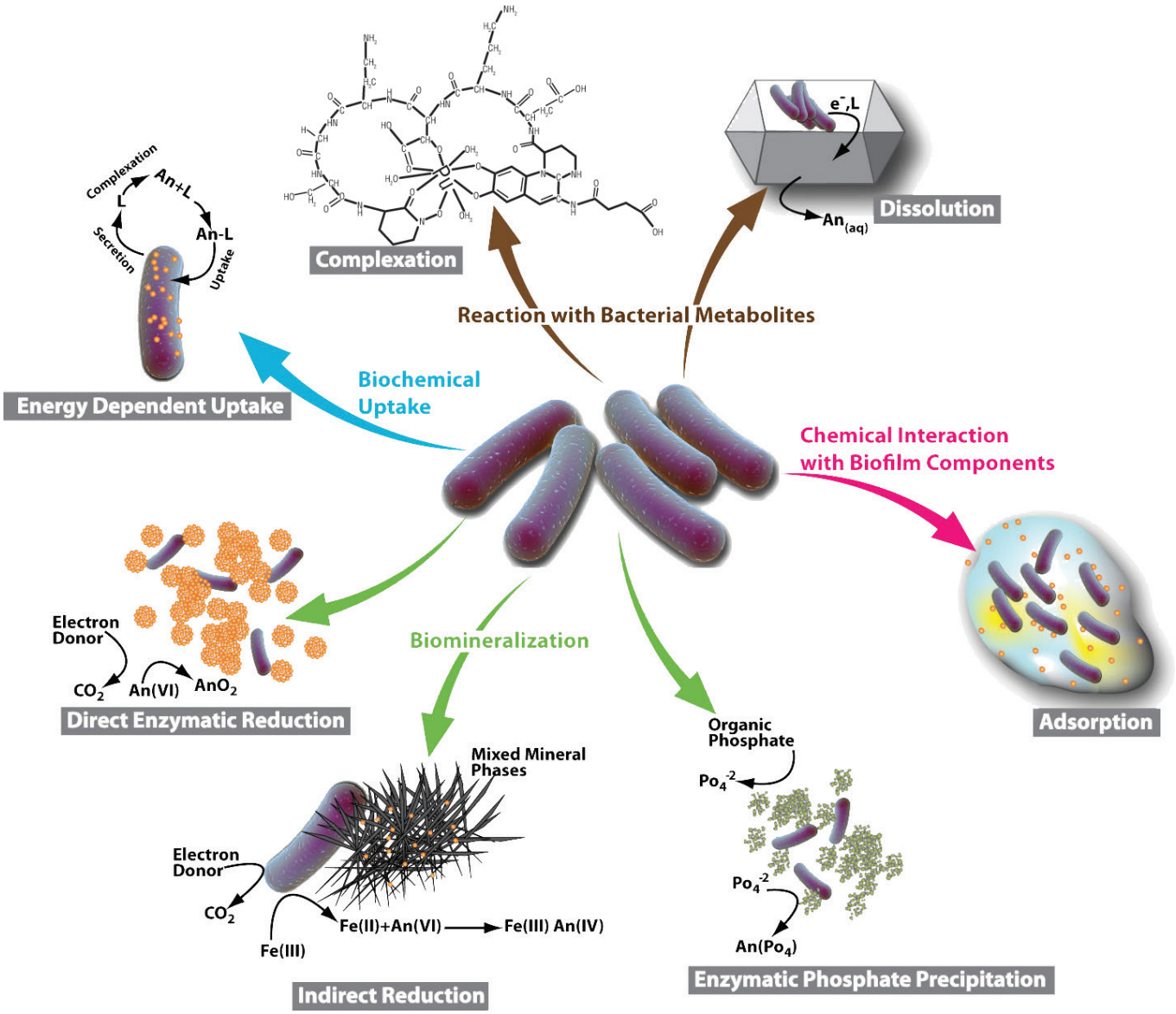

we reported in *Inorganic Chemistry* that the formation constant for Pu(IV)–DFB is log β = 33.98, which is about 1000 times higher than the constant for the Fe(III) complex and the Pu(IV)–H_2DFB_2 complex, which is log β = 62.3.

Because the Pu–siderophore complex is so stable, we proposed that it could be taken up by environmental bacterium. We first showed that *Microbacterium flavescens* (JG-9), a bacteria that does not produce any siderophore itself but is known to take up Fe(III)–DFB, can take up Pu(IV)–DFB. Building on those results, we showed that other types of bacteria take up the same amount of plutonium at rates similar to those at which they take up nutrient iron, even when complexes of both metals are present. We have found this is a general phenomenon: bacteria take up Pu(IV) via the same siderophore-mediated process that they use to internalize iron, whether

Acknowledgments

The research was performed for the Department of Energy, Office of Science, Biological and Environmental Research, using project funding in 1998–2007. The co-authors were postdoctoral researchers working with mentor Mary Neu in the Chemistry Division at Los Alamos National Laboratory, partially funded by the Los Alamos Glenn T. Seaborg Institute.

the siderophore is a hydroxamate or is comprised of other metal-binding functional groups. Interestingly, in experiments where the siderophore was present in greater than two-fold excess, Pu(IV) uptake decreased or was inhibited, whereas Fe(III) uptake was not. We proposed that this is because plutonium forms 2:1 ligand-to-metal complexes not recognized by cell membrane receptors that have evolved to take up the structurally distinct 1:1 Fe(III)–siderophore complex.

This year, Kersting and coworkers published NMR spectroscopic confirmation of the 2:1 plutonium complex in the European *Journal of Inorganic Chemistry*. It is not yet known where plutonium is stored inside the cell. An hypothesis, consistent with Pu(IV) being recognized and then shuttled into bacteria by processes the bacteria developed for Fe(III), is that internalized plutonium is incorporated into complex organic/inorganic clusters such as the iron storage protein ferritin. Consistent with this theory, Jensen's group at Argonne National Laboratory reported in 2011 in *Nature Chemical Biology* that plutonium can mimic iron interactions with mammalian Fe–protein complexes.

We broadened our studies of plutonium uptake by bacteria to examine several other actinide–bacteria interaction mechanisms. For example, we found that uranium and plutonium are generally less toxic to bacteria than are certain heavy metals such as Cd(II), Cr(VI), and Pb(II). We have shown that dissimilatory metal-reducing bacteria, *Shewanella* and *Geobacter* sp., reduce the actinides plutonium and uranium to nanocrystalline oxides, just as they do the transition metals iron and manganese. This mechanism is another way that bacteria bring actinides into cells. Several other mechanisms, such as enzyme transformation, polysaccharide binding, phosphate mineralization, and others concentrate actinides outside the cell. Most of the resulting products have not yet been characterized in detail.

During 2014, the International Year of Crystallography, it was appropriate to assess our progress in crystallographic studies of plutonium. By one measure, entries in the Cambridge Structural Database (CSD), a great deal of progress has been made in the last 15 years. In 2000, when we determined the structure of Pu–DFE, the CSD included 16 entries that contained plutonium, all limited to lattice parameters; none had 3D coordinates. The CSD now has about 100 plutonium entries, including a broad range of air-stable and air-sensitive compounds. A large portion of these compounds have been synthesized and characterized at Los Alamos.

Further Reading

Neu, M. P.; Icopini, G. A.; Boukhalfa, H. Plutonium Speciation Affected by Environmental Bacteria. *Radiochim Acta.* **2005**, *93(11)*, 705–714.

M. P. Neu; Ruggiero, C. E.; Francis, A. J. The Bioinorganic Chemistry of Plutonium. In *Advances in Plutonium Chemistry*; Hoffman, D. C., Ed., American Nuclear Society: LaGrange Park, Illinois, 2002, pp 169–211.

Runde, W. H.; Neu, M. P. Actinides in the Geosphere. In *The Chemistry of the Actinide Elements*, Katz, Seaborg, Morss, and Fuger, Eds.; Volume 3; Springer: The Netherlands, 2010, pp 1–59.

Neu, M. P.; Boukhalfa, H.; Merroun, M. L. Biomineralization and Biotransformations of Actinide Materials. *Mater. Res. Soc. Bull.* **2010**, *35(11)*, 849–857. Lead article in issue devoted to Future Actinide Research.

Structural Characterization of Actinide Iodates

This article was contributed by Wolfgang H. Runde, Science Program Office, Office of Science; and Amanda C. Gibbs, Proliferation Threat Analysis Group, both at Los Alamos National Laboratory.

The iodate anion IO_3^- forms a large class of inorganic structures with transition metals and lanthanides that are of broad interest because of their diverse coordination chemistries, magnetic properties at low temperatures, and usability as model materials to investigate hydrogen bonding in hydrated iodate compounds. The synthesis and crystal growth of 4*f* lanthanides is driven by the search for new optical-magnetic properties; the search for new 5*f*-element compounds is motivated by the need for radiation-resistant and insoluble materials suitable for safe long-term nuclear material storage. However, only a handful of iodates have been prepared with the sufficient crystal quality necessary for a full structural characterization. Common oxo-anionic compounds of hexavalent actinides, e.g., SO_4^{2-}, CO_3^{2-}, NO_3^-, PO_4^{3-}, are highly soluble in acidic media, but iodate anions offer the unique capacity to precipitate actinides even under mildly acidic conditions. In fact, iodate precipitation was used for oxidation state determination of plutonium in October 1942. Plutonium(IV) was precipitated from HNO_3 solutions upon addition of HIO_3 or KIO_3; however, the exact compositions of the precipitates remain unknown. The calculated molecular weight did not match the suggested formula, $Pu(IO_3)_4$, which indicated the possible presence of KIO_3 or HIO_3 in the solid.

Despite the early interest in 5*f* iodates for analytical and separation applications, little quantitative information on thermodynamic or structural properties of transuranic iodates is available. There are reports on the preparation and structural characterization of U(VI), Np(V), and Np(VI) iodates, whereas iodates of Pu(V), Pu(VI), and Am(III) have remained unexplored. We expanded the structural variety of f-element iodates from the 4*f* series to the 5*f* series by the synthesis of a novel open-framework Am(III) iodate, $K_3Am_3(IO_3)_{12}{\bullet}HIO_3$, and a new anhydrous Am(III) iodate, β-$Am(IO_3)_3$. Both these compounds exhibit structure types unprecedented in the lanthanide series. We also synthesized several novel U(VI), Pu(VI), and Np(VI) binary and ternary iodate compounds.

> ***"We expanded the structural variety of f-element iodates from the 4f series to the 5f series by the synthesis of a novel open-framework Am(III) iodate and a new anhydrous Am(III) iodate."***

$K_3Am_3(IO_3)_{12}{\bullet}HIO_3$

The most intriguing f-element iodate compound we synthesized is the open-framework Am(III) iodate, $K_3Am_3(IO_3)_{12}{\bullet}HIO_3$. Although hydrothermal conditions have been applied to the synthesis of transition metal, lanthanide, and light actinide (uranium, neptunium, plutonium) compounds, americium has been largely excluded from this approach because of safety and contamination concerns and the increased instability of americium crystals caused by α self-radiation damage. We overcame these difficulties and reacted ^{243}Am(III) in 3 M HCl with KIO_4 solutions at 180 °C for 24 hours. Although the high oxidation potential of the periodate anion in acid ($E°$ (IO_4^- / IO_3^-) = 1.65 V) oxidizes Pu(IV) completely to the hexavalent

state (E° (Pu^{4+}/PuO_2^{2+}) = 0.98 V), no oxidation of Am(III) to Am(VI) (E° (Am^{3+}/AmO_2^{2+}) = 1.69 V) was observed. Pink crystals within large amounts of colorless salts formed with nearly quantitative removal of americium from solution. The x-ray crystal structure analysis revealed the crystalline product to be $K_3Am_3(IO_3)_{12}•HIO_3$. This was the first actinide(III) iodate compound to be structurally characterized. It represents a single crystal architecture of an f-element iodate compound that has not been observed with lanthanide elements. The most interesting aspect of the compound derived from this work lies within the microporous channel framework and its potential application for cation exchange and catalysis.

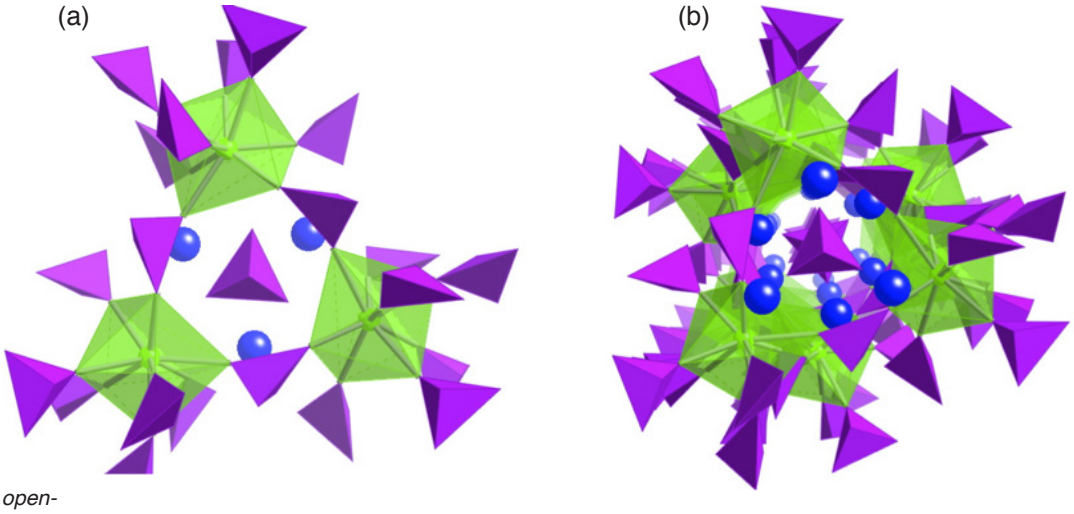

The authors synthesized a novel open-framework Am(III) iodate. Shown in (a) is a view of one segment of $K_3Am_3(IO_3)_{12}•HIO_3$. In (b) is a view along the K^+ (blue)-lined channel of $K_3Am_3(IO_3)_{12}•HIO_3$ formed along the c axis and built from alternating [AmO_8] polyhedra (green) and three [$I(5)O_3$] groups (purple) with neutral HIO_3 (purple) staggered in the channel center. The irregular hexagonal channels are about 4.6 Å in diameter.

Structure of $K_3Am_3(IO_3)_{12}•HIO_3$

The structure of $K_3Am_3(IO_3)_{12}•HIO_3$ consists of a three-dimensional arrangement of [AmO_8] units bridged by corner-sharing [IO_3] pyramids. Four unique crystallographic IO_3^- anions possess one terminal oxygen atom, with the remaining oxygen atoms bonding in a monodentate fashion to one metal center, while also serving to bridge two americium atoms. Each iodine atom from the unique IO_3^- anions forms an independent trigonal pyramid with three close oxygen atoms but deviates significantly from *3m* point symmetry. The distortion of the [$I(2\text{-}5)O_3$] pyramids is characterized by a wide range of short I–O bonds between 1.75(3) and 1.85(3) Å and O–I–O angles between 88(1) and 101(1)°, still within the expected ranges of bond lengths and angles for IO_3^- groups. In addition, there are three weak I---O interactions at longer distances from 2.67 to 3.01 Å, as found in other transition metal and lanthanide iodates.

Three [AmO_8] polyhedra and three [$I(5)O_3$] groups are arranged along the *c* axis to form irregular hexagonal channels about 4.6 Å in diameter. The [$I(3)O_3$] and [$I(4)O_3$] units link the tubes together to form a three-dimensional network, whereas [$I(2)O_3$] groups add additional connection and stability to the channel periphery. The potassium atoms line the

cavity with close contacts between the oxygen(1) and potassium atoms of 2.40(4) Å. Additional interactions between potassium atoms and four oxygen atoms from three of the four bridging IO_3 groups (K---O between 2.53 and 2.78 Å) indicate a complex three-dimensional bonding network. Neutral $HI(1)O_3$ molecules are staggered in the center of the void. The highly symmetrical HIO_3 pyramids contain three short I(1)–O(1) bonds of 1.92(4) Å and have an averaged O–I–O angle of 88.2(2)°. Six additional oxygen atoms originating from the three $[I(5)O_3]$ units are less than 3.3 Å apart, i.e., I(1)---O(11) = 2.86 Å and I(1)---O(13) = 3.24 Å. The oxygen–oxygen distances of 2.74 Å in the pyramidal plane of $[I(1)O_3]$ are within those found for the O–O distances in the bridging iodate groups (2.52–2.78 Å).

The americium $[AmO_8]$ polyhedra have eight $[IO_3]$ oxygen atoms to complete a distorted bicapped trigonal prismatic coordination. The Am–O distances range between 2.42(3) and 2.60(3) Å, which are similar to those observed in reported Ln(III) iodate compounds. In addition, one longer Am–O(1) distance of 2.93(4) Å is observed for the weaker interaction of the americium atom with the nearest oxygen atom of the neutral HIO_3 molecule. It follows that all nine oxygen atoms complete a distorted tricapped trigonal prismatic americium coordination sphere.

The most interesting aspect of the Am(III) iodate derived from this work lies within the microporous channel framework and its potential application for cation exchange and catalysis. It has not yet been determined whether the trapped neutral molecules can be replaced by other molecules varying in size and shape and whether the replacement of potassium cations along the channel exterior will affect the retention strength of the trapped molecules. The microporous channel framework structure offers the possibility of the synthesis of new microporous iodates of the chemically analogous trivalent lanthanides with unique selectivity properties for ion-exchange, catalysis, and photochemical processes. Only about a dozen single-crystal structures of americium compounds are reported in the literature. As demonstrated in $K_3Am_3(IO_3)_{12}{\bullet}HIO_3$, the rich coordination chemistry of americium may vary from its chemically analogous lanthanides and offers new insight into the differences in bonding of 4*f* and 5*f* elements.

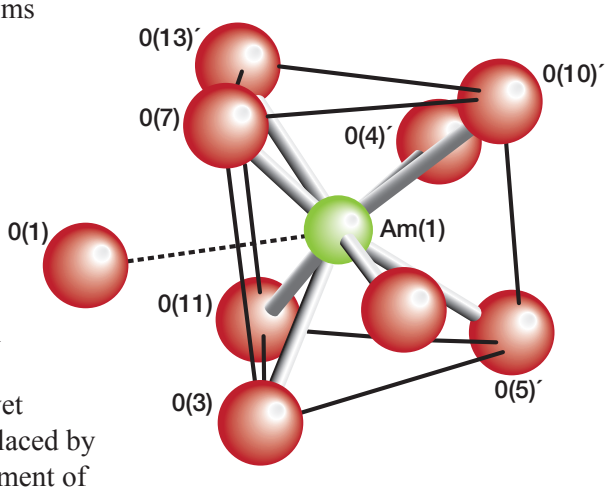

Reacting $^{243}Am(III)$ in 3 M HCl with KIO_4 solutions at 180 °C for 24 hours resulted in the first actinide (III) iodate compound to be structurally characterized. Shown here is the coordination environment of Am^{3+} in $K_3Am_3(IO_3)_{12}{\bullet}HIO_3$.

Anhydrous Lanthanides

The largest structural diversity belongs to the anhydrous lanthanides, $Ln(IO_3)_3$, which were found to precipitate in six different structure types. By reacting KIO_4 with $^{243}Am(III)$ in 0.1 M HCl in a polytetrafluoroethylene-lined autoclave at 180 °C for 72 hours, we obtained light orange crystals up to 0.2 mm in length, accompanied by nearly quantitative removal of americium from the solution. X-ray crystal structure analysis revealed the light orange product to be an anhydrous binary Am(III), β-$Am(IO_3)_3$, with a structure quite different from the known Type I (centrosymmetric monoclinic) structure. Type I anhydrous binary f-element iodates consist of a three-dimensional network of molecular $[MO_8]$ polyhedra that are solely connected by monodentate $[IO_3]^-$ groups.

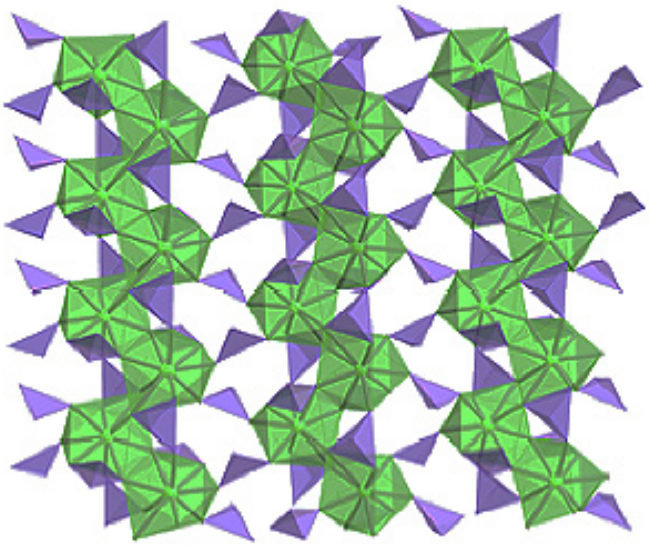

The authors synthesized a new anhydrous Am(III) iodate. Shown here is a polyhedral representation of the structural features in β-$Am(IO_3)_3$ as an illustration of $[I(3)O_3]$-connected zig-zag chains of $[AmO_9]$ polyhedra in the $Am_2(IO_3)_3$ layer.

In contrast, the structure of β-$Am(IO_3)_3$ consists of corrugated $[Am(IO_3)_3]$ layers that are arranged along the crystallographic *b* axis. Besides lower dimensionality, the most significant structural differences from the Type I f-element iodates are the higher coordination number of the americium ions and the more complex coordination modes of the iodate ligands in β-$Am(IO_3)_3$. A combination of edge-sharing and corner-sharing $[IO_3]$ groups permits the coordination of only seven ligands using nine oxygen atoms to define a distorted tricapped trigonal prism around the americium center. The β^2-$[I(1)O_3]$ group is bidentately coordinated to one americium atom via O(1) and O(7) with the terminal O(8) atom pointing toward an adjacent layer. The β^3-$[I(2)O_3]$ group stabilizes the $[AmO_9]$ ribbon by sharing its three oxygen atoms with three adjacent americium atoms. Both iodate atoms, I(1) and I(2), sustain a zig-zag chain of $[AmO_9]$ polyhedra along the *b* axis. The two-dimensionality is created by β^2-$[I(3)O_3]$ groups that link two adjacent $[AmO_9]$ chains using O(2) and O(6) to form an extended layer along the *b* axis. The terminal O(3) atom is arranged to point toward the neighboring $Am(IO_3)_3$ layer. All $[IO_3]$ groups exhibit the expected trigonal pyramidal configuration of I(V) with three short I–O bond distances between 1.81 and 1.84 Å. Each iodine atom has three further oxygen atom neighbors at longer distances between 2.39 and 3.00 Å in a highly distorted octahedron. The short I--O distance of 2.39 Å has been observed only in β–KIO_3-HIO_3, whereas similar long-range I---O contacts have been found in many transition metal and lanthanide iodates (ranging between 2.5 and 3.2 Å). The I(2) and I(3) octahedra are connected using the O(4) and O(6), respectively, to form infinite $[IO_6]$ chains along the *b* axis. However, the $I(1)O_3$ groups form $[I_2O_{10}]$ dimeric moieties with one short (1.839 Å) and one long (2.390 Å) distance between I(1) and the β^2-O(8) atom. This close arrangement that is unique within thus-far-reported f-element iodates creates a pseudo-three-dimensional connection between the $Am(IO_3)_3$ layers.

The americium [AmO_9] polyhedra have nine [IO_3] oxygen atoms that complete a distorted tricapped trigonal prismatic coordination. The eight Am–O distances range between 2.398(7) and 2.676(8) Å, and are similar to the distances observed in the Type I Am(III) iodate compound (2.34–2.60 Å). In addition, one longer Am–O(5) distance of 2.823(8) Å is observed, as found in the nine-coordination of americium in $K_3Am_3(IO_3)_{12}•HIO_3$. The triangular linkage of [AmO_9] polyhedra by [$I(1)O_3$] and [$I(2)O_3$] groups creates very close Am–Am distances of 4.252, 4.527, and 5.932 Å, which are significantly smaller than the closest Am–Am distances found in β-$Am(IO_3)_3$ (5.957, 6.057, and 7.243 Å).

The α-$Am(IO_3)_3$ Form

In contrast to the β-form, the α-$Am(IO_3)_3$ form consists of a three-dimensional network of molecular [AmO_8] polyhedra that are solely connected by monodentate [IO_3] groups. Consequently, the eight oxygen atoms around the one americium atom that is crystallographically uniquely positioned originate from eight iodate ligands forming a distorted dodecahedral coordination sphere. The eight Am–O distances range between 2.34(1) and 2.60(1) Å, and are slightly extended compared with the Ln(III)–O distances in $Gd(IO_3)_3$ and $Tb(IO_3)_3$. Three crystallographically distinct trigonal pyramidal iodate groups serve to link the americium atoms and show only slight variations in their I–O bond distances (1.77 and 1.84 Å). The μ^2-[$I(1)O_3$] group bridges two adjacent [AmO_8] polyhedra through O(13) and O(14) with I(1)–O bond distances of 1.77 Å for O(13) and 1.78 Å for O(14); a bond distance to the terminal O(12) atom of 1.77 Å is observed. The μ^3-[$I(2)O_3$] group with I(2)–O bond distances between 1.77 and 1.83 Å bridges three [AmO_8] polyhedra to form zig-zag layers in the *ab* plane similar to those found in β-$Am(IO_3)_3$. The combination of [$I(1)O_3$] and [$I(2)O_3$] groups ensures a three-dimensional connection of the [AmO_8] polyhedra. The μ^3-[$I(3)O_3$] group also bridges three [AmO_8] polyhedra connecting americium atoms in the *bc* plane. The I–O distances in [$I(3)O_3$] range from 1.78(3) to 1.80(3) Å. The averaged iodine–oxygen bond distance of 1.797 Å agrees well with the averaged iodine–oxygen bond distance of 1.80 Å in $Gd(IO_3)_3$. Each iodine atom shares two (I(1)---O = 3.02 and 3.04 Å) or three (I(2,3)---O = 2.72 – 3.08 Å) additional oxygen atoms from other [IO_3] groups, with the I---O distances significantly elongated compared with those in β-$Am(IO_3)_3$.

We used conventional ultraviolet-visible-near infrared diffuse reflectance spectroscopy to verify the oxidation state of the americium ion. The electronic absorbance spectrum for Am^{3+}(aq) is dominated by the well-known absorbance at 503 nm. This characteristic band is shifted to about 508 nm with a shoulder at 516 nm in the diffuse reflectance spectrum of $Am(IO_3)_3$, which confirms the trivalent oxidation state and strong coordination of the americium ion. It is still unclear why the absorbance

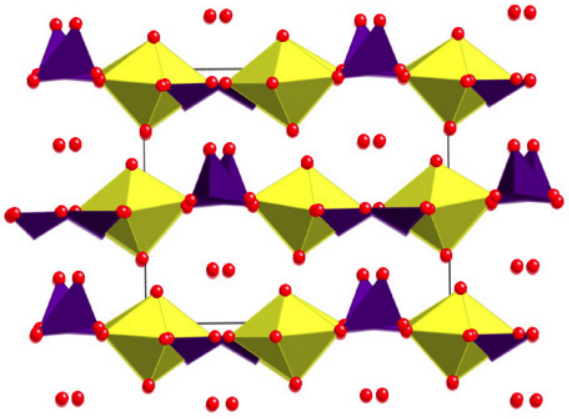

When characterizing the structures of hydrated plutonium iodates, we found water molecules beween layers of [IO_3] and [PuO_7] units. Shown here to illustrate the arrangement of layers and lattice waters is a view down the a *axis of plutonyl polyhedra and iodate pyramids of $PuO_2(IO_3)_2•H_2O$.*

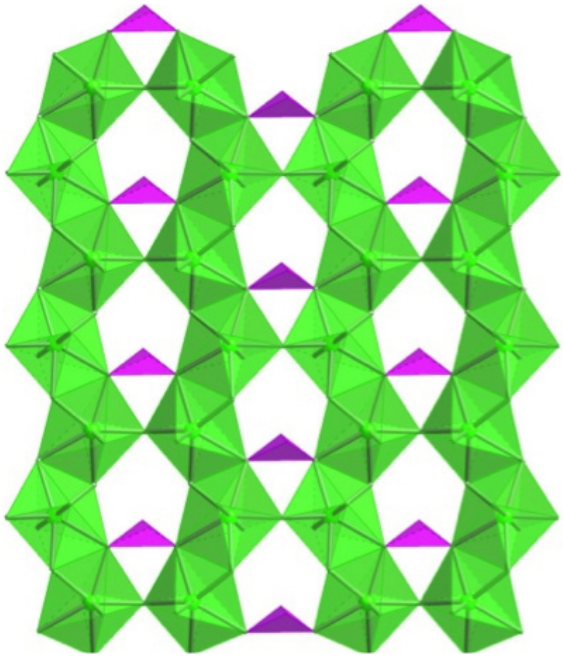

View of the infinite two-dimensional ribbons that run down the a *axis of $(PuO_2)_2(IO_3)(OH)$. The ribbons are formed from edge-sharing $[PuO_7]$ polyhedra and are linked by bridging $[IO_3]$ groups and OH ligands.*

shift is less than in other Am(III) compounds with bidentately coordinated ligands, such as in $Am(CO_3)_3^{3-}$ (509 nm). The Raman frequencies of β-$Am(IO_3)_3$ are quite different (737, 753, 784, and 814 cm^{-1}) from those in β-$Am(IO_3)_3$ (761, 803, and 845 cm^{-1}) and β-$Nd(IO_3)_3$ (764, 808, and 850 cm^{-1}) in which the frequencies for one symmetric and two asymmetric I–O stretching modes are observed at 761, 803, and 845 cm^{-1} for α-$Am(IO_3)_3$.

Neptunium and Plutonium Iodates

Similar staggered layers can be found in Np(V,VI) and Pu(VI) iodate compounds that formed under hydrothermal conditions at pH = 0, with water molecules arranged between the layers. The layers are built from corner-sharing $[IO_3]$ and $[PuO_7]$ units. The plutonium $[PuO_7]$ polyhedra comprise two trans-oxygen atoms with an O=Pu=O angle of 178.9(4)° and five $[IO_3]$ oxygens atoms in the equatorial plane to complete a slightly distorted pentagonal-bipyramidal coordination. The averaged Pu=O bond length of 1.75(1) Å compares well with those found by x-ray absorption spectroscopy for other Pu(VI) compounds, such as 1.74(1) Å in the PuO_2^{2+} aquo ion or in (K-18-crown-6)$_2PuO_2Cl_4$. The oxidation state of plutonium was confirmed by the characteristic peak of Pu(VI) at about 830 nm in the diffuse reflectance and in the absorbance spectrum of $PuO_2(IO_3)_2 \cdot H_2O$ when dissolved in $HClO_4$. The Pu–O distances in the equatorial plane range from 2.332(7) to 2.418(8) Å and are similar to those observed in reported U(VI) iodate compounds. Each plutonium atom is bridged by five iodate ligands to six other plutonium atoms with bridging of two and three plutonium atoms. Bidentate chelation of IO_3^-, as found in anhydrous $UO_2(IO_3)_2$, is absent in the hydrated Pu(VI) iodates we synthesized.

To obtain ternary Pu(VI) iodates, e.g., the hydroxo-iodato compound $(PuO_2)_2(IO_3)(OH)_3$, we reacted Pu(IV) with KIO_4 at pH = 8 at 180 °C for 48 hours. The high oxidation potential of the periodate anion ($E°$ (IO_4^- / IO_3^-) = 1.65 V) oxidizes Pu(IV) completely to the hexavalent oxidation state ($E°$ (Pu^{4+}/PuO_2^{2+}) = 0.98 V). Red-brown rectangular crystals formed with nearly quantitative removal of plutonium from solution. The most interesting element of this structure is the linkage of plutonium atoms by hydroxo and iodate groups. Each bridging oxygen atom from the iodate groups shares two plutonium atoms, which results in the coordination of four metal centers by only two iodate oxygen atoms. Also, the $[PuO_7]$ polyhedra are connected by bridging hydroxo groups, which are uncharacterized for Pu(VI) compounds. The Pu–OH distances in the equatorial plane between 2.342(9) and 2.390(9) Å are attributed to the μ_3-OH ligand in the edge-sharing intra-chain linkage. The shortest Pu–O distances of 2.277(9) Å for Pu(1) and 2.308(9) Å for Pu(2) correlate to the O(8) atom of the corner-sharing $[PuO_7]$ polyhedra of adjacent chains. The presence of μ_2-OH groups illustrates that Pu(VI) displays a rich coordination chemistry that is comparable to that of U(VI).

Further Reading

Runde, W.; Bean, A. C.; Scott, B. L. Synthesis and Characterization of a Channel Framework in $K_3Am_3(IO_3)_{12} \cdot HIO_3$. *Chem. Commun.* **2003**, 1848. Advance article on Web, Aug. 7, 2003.

Runde, W.; Bean, A. C.; Brodnax, L. F.; Scott, B. L. Synthesis and Characterization of f-Element Iodate Architectures with Variable Dimensionality, α- and β-$Am(IO_3)_3$. *Inorg. Chem.* **2006**, *45*, 2479–2482.

Bean, A. C.; Scott, B. L.; Albrecht-Schmitt, T. E.; Runde, W. Structural and Spectroscopic Trends in Actinyl Iodates of Uranium, Neptunium, and Plutonium. *Inorg. Chem.* **2003**, *42*, 5632–5636.

Runde, W.; Bean, A.; Albrecht-Schmitt, T. E.; Scott, B. L. Synthesis and Characterization of a Channel Framework in $K_3Am_3(IO_3)_{12} \cdot HIO_3$. *Chem. Commun.* **2003**, *15*, 1848–1849.

Bis(imido) Uranium (VI) Complexes: The First Imido Analogs of the Uranyl Ion

Nitrogen Analogs of the Uranyl Ion

This article was contributed by James M. Boncella, Inorganic Isotope and Actinide Chemistry, Los Alamos National Laboratory.

Introduction

The uranyl ion [*trans*-O=U=O]$^{2+}$ is the most common molecular complex of uranium and has been known for over 150 years.[1] Species with this structure are involved in all aspects of uranium processing, encompassing the extraction of uranium from ores, the synthesis and reprocessing of nuclear fuel, and the disposition of nuclear waste, including the fate and transport of uranium in the environment. These compounds are characterized by the *trans*-dioxo structure as shown below.

NOTE: Throughout this article, the U=O and U=NR multiple bonds are written with two lines to account for the valence at the metal center even though analysis of the orbital interactions between the uranium and nitrogen or oxygen atoms indicates that, in both cases, these interactions are best described as metal-ligand triple bonds.

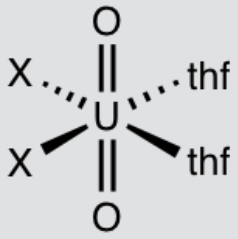

The trans*-dioxo structure is unusual for metal-dioxo complexes and arises because of the participation of the 5f valence orbitals in the U=O bonding within imido analogs of the uranyl ion.*

Isoelectronic nitrogen (imido) analogs of the uranyl ion have been of interest to actinide chemists for many years because of the potential to modify the chemistry of species such as this by tuning the nitrogen substituents, R_2. With general synthesis of bis(imido) analogs of the uranyl ion, changes in the steric and electronic properties of the NR substituents have the potential to produce compounds with new modes of reactivity. This in turn would lead to better understanding of actinide-light atom bonding in general.

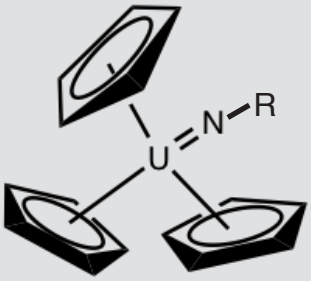

Attempts to synthesize $[U(=NR)_2]^{2+}$ complexes by modification of the parent uranyl ion have been unsuccessful, most likely because of a combination of the thermodynamic stability of the U=O interaction and its kinetic inertness. The first example of a complex containing a uranium-nitrogen multiple bond as shown here was reported in 1985 by Brennan and Andersen.[2]

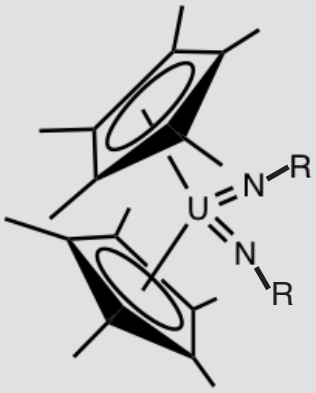

The synthesis of U(VI)bis(imido) complexes such as $[U(=NR)_2]^{2+}$, as shown here, was first reported from Los Alamos by Burns and co-workers in 1992,[3] but these compounds did not have imido groups that were trans *to one another on the metal center.*

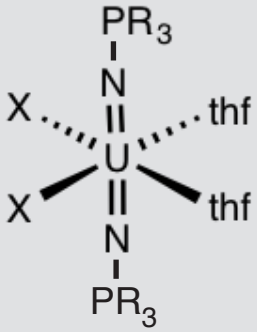

Later, the trans*-bis(phosphiniminato) complexes were successfully synthesized,[4] but even with the stabilizing phosphorus substituents, their extremely reactive nature led to the prediction that* trans*-(bis) imido complexes of U(VI) having simple alkyl or aryl substituents on the imido nitrogen would be unstable to reduction and impossible to isolate.[2]*

In 2005, we were surprised and pleased to discover that the oxidation of uranium metal with iodine in the presence of $^{t}BuNH_2$ gives the bis(imido) U(VI) complex, Eq. 1.[5] This reaction is a simple, high-yielding procedure for the synthesis of a long-sought-after nitrogen (imido) analog of the ubiquitous uranyl ion. The bis(imido)U(VI) complex includes a simple, nonstabilizing, alkyl substituent on nitrogen as well as the crucial *trans*-disposition of the imido groups. It was clear that this compound presented not only the opportunity to gain further insight into the bonding between uranyl and its analogs but also the potential to access new horizons in uranium chemistry by exploring a novel class of U(VI) complexes.

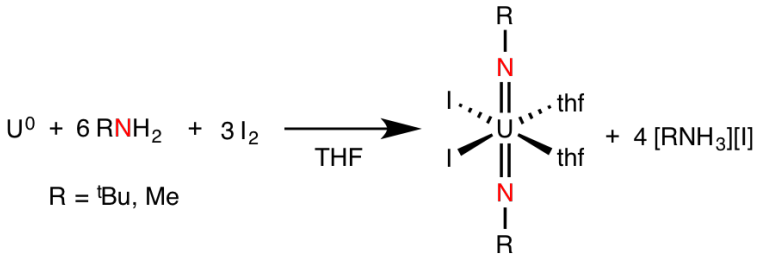

(1)

The reaction in Eq. 1 involves the installation of the U=N multiple bond through an oxidation reaction rather than modification of the uranyl ion. This further emphasizes the thermodynamic and kinetic stability of the *trans*-dioxo uranium functionality. The successful use of iodine as an oxidant in these reactions is notable and was initially somewhat surprising. Iodine is not a strong enough oxidant to access U(VI) by itself. UI_6 and UI_5 are both unknown and UI_4 is unstable with respect to disproportionation to UI_3 and I_2 in the absence of stabilizing Lewis bases. These observations clearly demonstrate that the formation of the U=N multiple bonds in the bis(imido) complexes provides a significant thermodynamic driving force for these oxidation reactions. Subsequent work has shown that the driving force for formation of the bis(imido)U(VI) moiety from lower valent uranium compounds defines the chemistry of the lower valent species, and creation of the U=NR unit is very facile under the correct conditions and can even be difficult to prevent.

Although the reaction in Eq. 1 gave access to the desired bis(imido)U(VI) complexes, it has been limited to R = ^{t}Bu or Me. Given that iodine reacts with uranium metal to give UI_3, we explored the possibility of synthesizing the U(VI)bis(imido) complexes by starting from UI_3 and discovered that oxidation of UI_3 with iodine in the presence of a primary amine and a base also gives the bis(imido)U(VI) complexes in excellent yields, Eq. 2.[6]

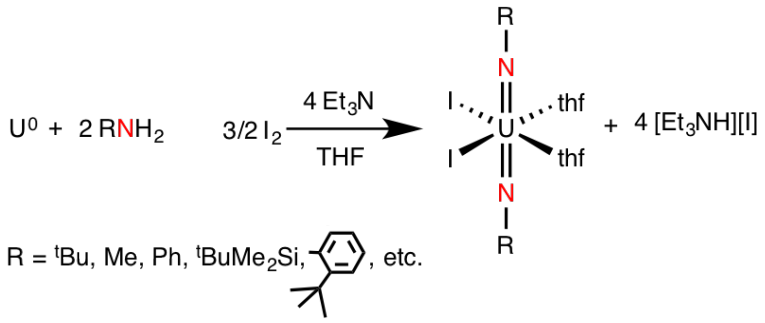

(2)

This reaction takes advantage of the thermodynamic driving force inherent in the formation of the U=N multiple bonds from lower valent uranium starting materials. Forming bis(imido)U(VI) compounds from UI_3 is far more versatile than using Eq. 1 and gives access to many imido complexes in which the nitrogen substituent has variable steric and electronic properties. With the synthetic protocols in Eq. 1 and Eq. 2 in hand, we have been able to explore and develop this new area of uranium chemistry.

Structures and Bonding Analysis

The structures of bis(imido)U(VI) compounds, as shown in the sidebar, are characterized by axial *trans*-imido groups and either four or five ligands in the equatorial plane leading to overall pseudo-octahedral or pentagonal bipyramidal coordination geometries at the metal center. The U=N bonds vary from about 1.85 to 1.91 Å, with the N=U=N angle being approximately linear, with angles ranging from about 165 to 180°. This compares to the uranyl ion that typically has U=O distances of about 1.76 to 1.78 Å and O=U=O angles very close to 180°. Density functional theory (DFT) calculations indicate that the *trans*-bis(imido)U(VI) structure is favored over the *cis*-bis(imido)U(VI) geometry by about 15 kcal/mol.[4] Furthermore, the calculated charges on the uranium atoms in these two classes of compounds show that there is less positive charge on the uranium in the imido species than in the uranyl ion. The smaller charge on the uranium atom in the U=NR compounds suggests that the uranium atom in the bis(imido) complexes should be a softer Lewis acid than in uranyl complexes.

In both sets of compounds, each U=E (E = O, N) bonding interaction is made up of one U–E σ bond and two U–E π bonds, thereby making the overall interaction that of a U=E triple bond. The U=NR interactions are significantly different from the U=O interactions. Specifically, the highest occupied bonding orbitals in the U=NR molecules consist of the U–N π interactions in which considerable electron density is localized on the nitrogen atom. In the case of uranyl compounds, the highest occupied orbital is actually a U=O σ interaction that is significantly lower in energy and less prone to reactivity than the U=N π interaction. The net result is that the U=NR bonds are significantly more reactive than the U=O bonds in the uranyl ion. These reactivity differences have enabled us to begin to better understand how metal ligand covalency in uranium compounds affects and controls reactivity.

Substitution Chemistry Comparison to Uranyl

Our initial reactivity studies revealed that the bis(imido)U(VI) species is indeed a softer Lewis acid than the uranyl ion. This was demonstrated by the observation that phosphine complexes are readily formed with $[(RN=)_2UI_2]$, Eq. 3,[6] while phosphine complexes of the uranyl ion have not been isolated or observed. Furthermore, the iodide or halide ligands in $[(RN=)_2UI_2(L)_2]$ can be readily substituted with a variety of anionic donor ligands, including soft donors such as RE^-, E=S, Se, Te.[7] Such simple chalcogenolate derivatives

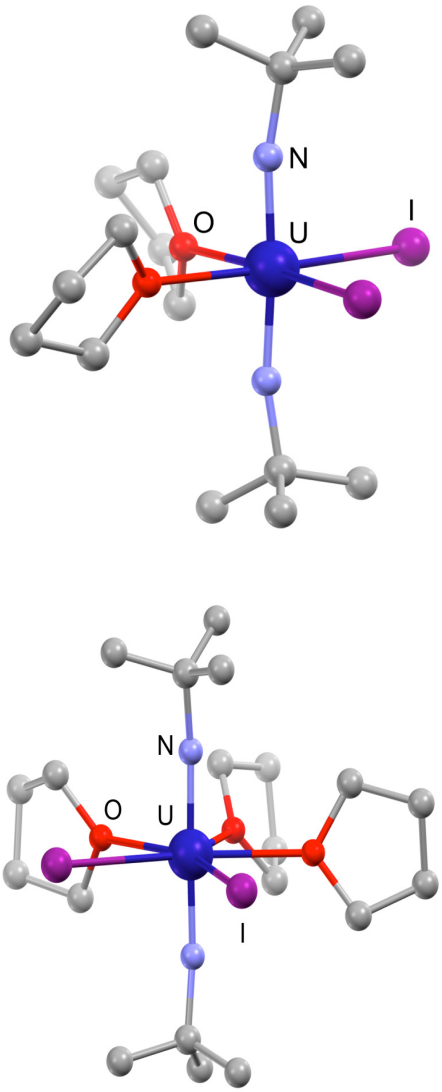

X-ray crystal structures of U(VI)bis(imido) complexes are characterized by axial trans- *imido groups and either four or five ligands in the equatorial plane leading to overall pseudo-octohedral or pentagonal bipyramidal coordination geometries at the metal center.*

of the uranyl ion have never been isolated, which shows the significant differences in chemistry that exist between these two structurally similar, but fundamentally different, metal species.

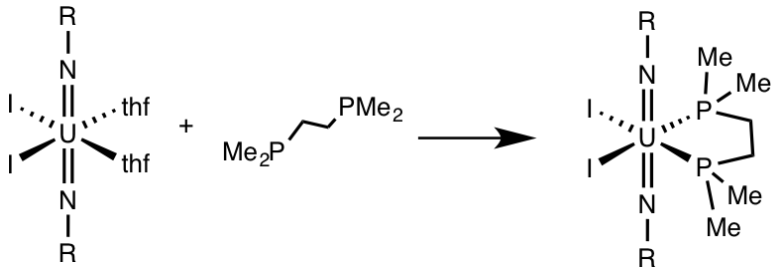

(3)

One of the most interesting demonstrations of the unique reactivity of the $[(RN=)_2U]^{2+}$ species is shown in Scheme 1.[8] In this reaction sequence, the first step involves the displacement of the iodide ligands and bipyridine ligands by sodium cyclepentadienide, NaCp, to generate the bis(cyclopentadienyl)U(=NR)$_2$ complex. In this compound, the N=U=N angle is 103°, and the U=N bond lengths are 1.93 Å, which is typical for this class of compounds. Surprisingly, this compound binds the bidentate phosphine ligand 1,2-bis(dimethylphosphino)ethane (DMPE), as shown in Scheme 1, to give the resultant compound shown. The coordination with the DMPE ligand causes the U–Cp bonds to lengthen considerably while the N=U=N angle expands to 154°. This reaction demonstrates the stability associated with the combination of a linear (or relatively linear) N=U=N angle and coordination of the metal to a soft donor phosphine ligand.

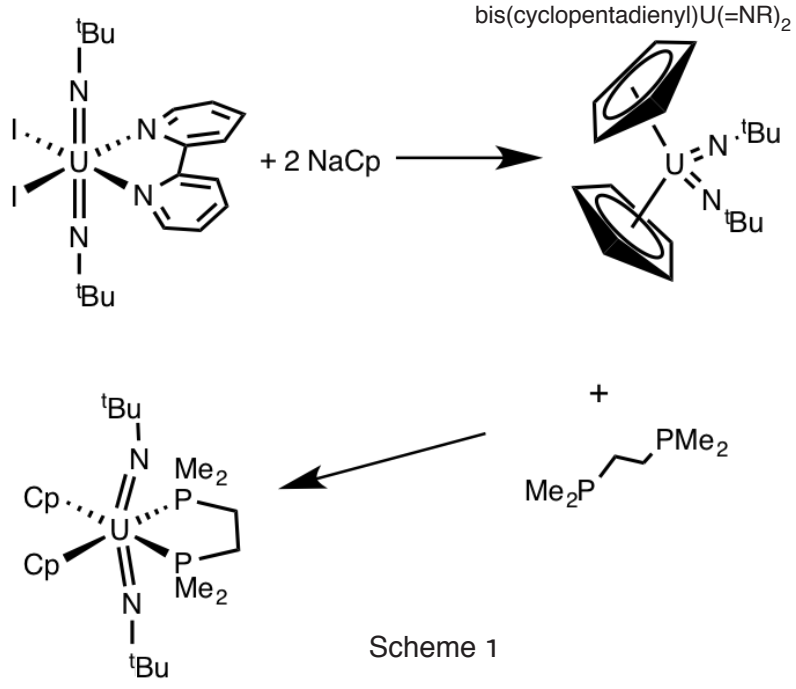

Scheme 1

Lower Valent Species

We were interested in accessing lower valent imido complexes of uranium. Although the synthesis of a genuine example of a bis(imido)U(IV) complex has proven elusive, we have discovered that mono(imido)U(IV) complexes are readily available, as shown in Eq. 4.[9,10]

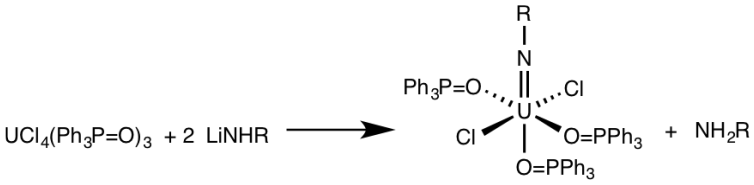

(4)

In this case, the formation of the U=N multiple bond occurs without oxidation of the metal center. The structures of the resultant imido complexes are highly dependent upon the co-ligands in the reaction. When strong Lewis bases such as bipyridine or triphenyl phosphine oxide are present, mononuclear complexes with terminal U=NR groups are formed. Under circumstances where only weaker Lewis bases are present, the isolated materials contain imido ligands that bridge two metal centers.[9] Reactions with four equivalents of $[HNR]^-$ reagent that might be expected to give a bis(imido)U(IV) product only give imido products that are higher valent materials than the isolable compounds. It appears that an unstable U(IV)bis(imido) complex, or a complex that behaves as if it were a U(IV)bis(imido) complex, is formed as an unstable intermediate in these reactions. This intermediate can be intercepted with added oxidants and has proven useful in the synthesis of U(VI)bis(imido) and U(V)bis(imido) complexes. Oxidation of this intermediate material with I_2 or another oxidant results in U(VI)bis(imido) complex products.[10] The procedure gives excellent yields of a variety of U(VI)bis(imido) complexes while using the readily available UCl_4 as the uranium starting material.

If the stoichiometry and oxidizing power of the oxidant is controlled, as shown in Eq. 5, then mononuclear bis(imido)U(V) complexes can be synthesized.[11] Because U(V) is still a rare oxidation state of uranium, these compounds promise to add greatly to our understanding of uranium chemistry in general and especially how redox transformations occur in uranium chemistry. Mononuclear bis(imido)U(V) complexes have longer U=N bonds than their analogous U(VI) counterparts, with average U(V)=NR distances of ~1.97 Å, depending upon the steric properties of the R group and co-ligands. The U(V) complexes complete the series of molecules of U(IV-VI) imido species with simple co-ligands and have enabled us to begin to investigate differences in bonding and reactivity of the U=NR functionality as a function of oxidation state.

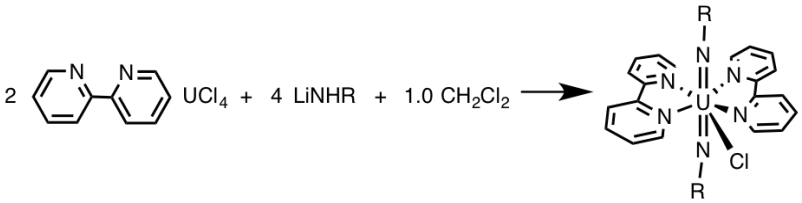

(5)

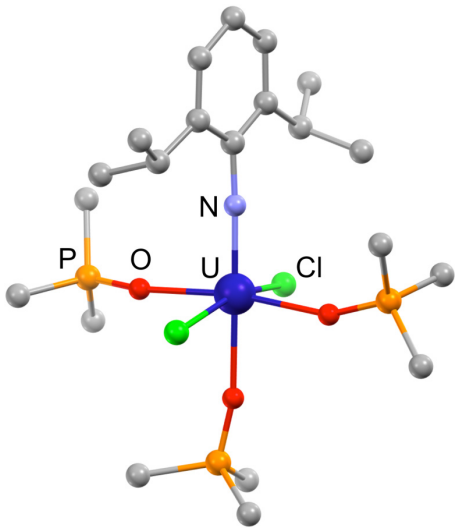

This is a model of an x-ray crystal structure of a U(IV)imido complex having a U=N bond length of 1.99 Å. Equation 4 shows an example of a mono(imido)U(IV) complex.

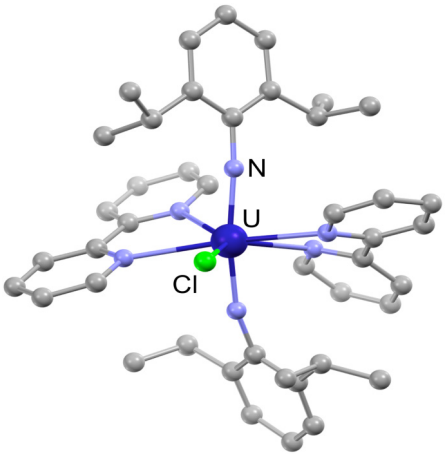

This model of an x-ray crystal structure of an unstable U(IV)bis(imido) complex shows an example of the complexes that can be synthesized, as shown in Eq. 5.

Reaction Chemistry of the Imido Groups

As mentioned above, the oxo groups of the uranyl ion are notoriously kinetically inert. The combination of thermodynamic stability and kinetic inertness is largely responsible for the ubiquitous nature of uranyl in uranium chemistry. The reasons for this are directly attributable to the electronic structure associated with the U=O bonds in these compounds. Perhaps the most obvious difference between the reaction chemistry of the uranyl ion and the U=NR compounds is the extreme sensitivity of U=NR materials to water regardless of oxidation state. Although uranyl ions are stable in aqueous solution, even traces of water will protonate the U=NR group at nitrogen, leading to the formation of amine and uranium oxo or hydroxo species. Controlled reaction of the U(VI)bis(imido) species and a stoichiometric amount of water leads to the formation of the mixed oxo-imido species that is the final product in Eq. 6.[12]

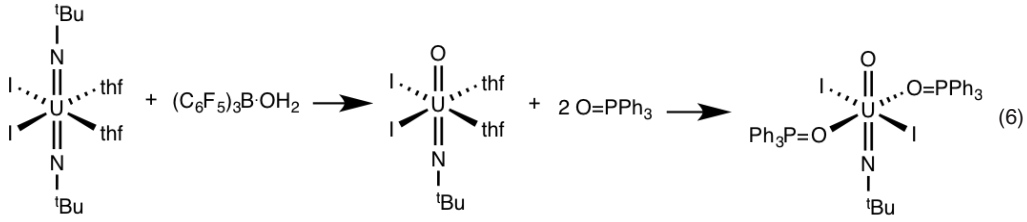

(6)

These compounds are functionally intermediate between uranyl ions and the bis(imido)U(VI) species. Interestingly, the U=N distances in these compounds are consistently the shortest that we have observed and are yet another experimental observation of the "inverse trans influence" that was first observed by Denning in mono-oxo U(VI) complexes.[13] DFT calculations on the oxo-imido compounds suggest that there is very little interaction between the bonding orbitals of the oxo and imido groups. These compounds offer a platform that can be used to investigate the reactivity and bonding of the oxo and imido groups in the same molecule.[12]

Electrophiles other than the proton also react with the U=NR groups in uranium imido compounds with interesting differences depending upon the oxidation state of the U=NR compound. As shown in Eq. 7, the reaction of U(VI)bis(imido) complexes with aryl isocyanate compounds at room temperature proceeds by exchange of the imido and isocyanate NR groups.[14]

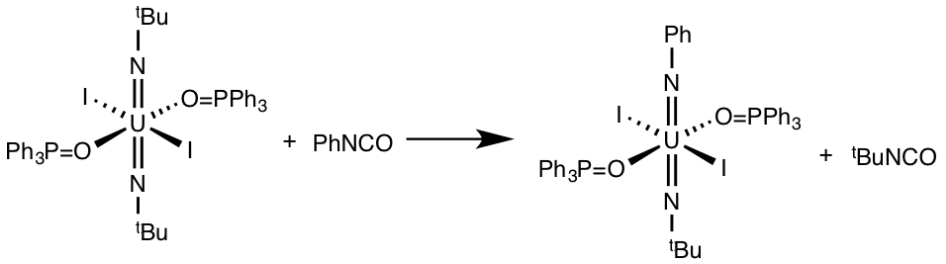

(7)

This exchange is the kinetic product of the reaction, since performing the reaction at elevated temperature results in the formation of the oxo-imido and uranyl complexes as products. The calculated energies of the two possible intermediates suggests that the observed reactivity arises because the U-N-C-N metallacycle, which leads to imido exchange, is lower in energy than the U-N-C-O metallacycle, which leads to oxo formation.[14]

The reaction of mononuclear U(IV)(=NR) compounds with aryl isocyantes proceeds by electrophilic attack of the isocyanate on the nitrogen atom, Eq. 8, but in this case, instead of imido exchange, the U-N-C-N metallacycle (U-ureate) complexes are the isolable products of the reaction.[15]

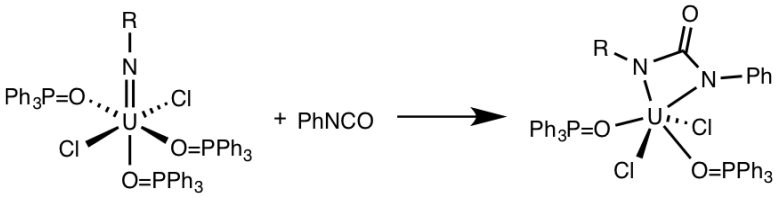

(8)

This observation is consistent with the suggestion that the U=NR group in the lower oxidation state is a stronger nucleophile. DFT calculations are consistent with this view, showing more negative charge buildup on the nitrogen atom and a greater positive charge on the uranium atom in the U(IV) compounds than in the U(VI) compounds. These differences in the U=NR bonding are directly attributable to differences in the uranium-nitrogen orbital interactions in these two oxidation states. Thus, the changes in reactivity that we see can be explained by differences in the covalency in the U=N bonds as a function of the metal oxidation state.

"The key to accessing bis(imido)U(IV) complexes is using lower valent uranium compounds as starting materials."

Summary and Conclusions

The synthesis of bis(imido)U(VI) complexes has allowed us to broaden and further develop the chemistry of uranium. The key to accessing this unique class of molecules is using lower valent uranium compounds as starting materials, thereby using the thermodynamic stability associated with the U=N bond to drive the reaction. We have found that uranium metal, U(III), and U(IV) precursors can all be suitable precursors in these syntheses, albeit under different conditions. These reactions provide convenient access to a wide variety of bis(imido)U(VI) compounds with different R groups. Comparison of these compounds with the ubiquitous uranyl complexes has revealed striking differences in reactivity and bonding despite the structural similarities between the uranyl and $[(RN=)_2U]^{2+}$ ions. The U=NR compounds are softer Lewis acids than their uranyl analogs, and the U=NR bond is much more reactive than the U=O bonds in uranyl compounds. We have used these differences to generate both unusual U-Lewis base adducts and novel uranium compounds formed when U=NR groups react with electrophiles. This reaction chemistry greatly expands the synthetic "toolkit" available for the generation of new uranium species.

The results from our initial studies on U(VI) imido formation have also been used to develop the synthesis of U(IV) and U(V) imido compounds. Investigation of the chemistry of these new species is resulting in new insights into the fundamental properties of uranium compounds, such as the effect of metal-ligand covalency on reactivity. Going forward, the synthetic procedures developed for uranium may also be applicable to transuranic elements, since some of the same starting materials can be used for neptunium and plutonium. It remains to be seen, however, whether the M=NR multiple bond is stable and isolable for the transuranic elements.

References

1. Comyns, A. E. The Co-ordination Chemistry of the Actinides. *Chem. Rev.* **1960**, *60*, 115.
2. Brennan, J. G.; Andersen, R. Electron-Transfer Reactions of Trivalent Uranium. *J. Am. Chem. Soc.* **1985**, *107*, 514.
3. Arney, D. J.; Burns, C. J.; Smith, D. C. Synthesis and Structure of the First Uranium(VI) Organometallic Complex. *J. Am. Chem. Soc.* **1992**, *114*,10068.
4. Brown, D. R.; Denning, R. G. Stable Analogs of the Uranyl Ion Containing the –N=U=N– Group. *Inorg. Chem.* **1996**, *35*, 6158.
5. Hayton, T. W.; Boncella, J. M.; Scott, B .L.; Palmer, P. D.; Batista, E. R.; Hay, P. J. Synthesis of Imido Analogs of the Uranyl Ion. *Science*, **2005**, *310*, 1941.
6. Hayton, T. W.; Boncella, J. M.; Scott, B. L.; Batista, E. R.; Hay, P. J. Synthesis and Reactivity of the Imido Analogues of the Uranyl Ion. *J. Am. Chem. Soc.* **2006**, *128*, 10549.
7. Spencer, L. P.; Yang, P.; Scott, B. L.; Batista, E. R.; Boncella, J. M. Uranium(VI) Bis(imido) Chalcogenate Complexes: Synthesis and Density Functional Theory Analysis. *Inorg. Chem.* **2009**, *48*, 2693.
8. Spencer, L. P.; Gdula, R. L.; Hayton, T. W.; Scott, B. L.; Boncella, J. M. Synthesis and Reactivity of Bis(imido) Uranium(VI) Cyclopentadienyl Complexes. *Chem. Comm.* **2008**, 4986.
9. Jilek, R. E.; Spencer, L. P.; Kuiper, D. L.; Scott, B. L.; Williams, U.; Kikkawa, J. M.; Schelter, E. J.; Boncella, J. M. A General and Modular Synthesis of Monoimidouranium(IV) Dihalides. *J. Inorg. Chem.* **2011**, *50*, 4235.
10. Jilek, R. E.; Tomson, N. C.; Shook, R. L.; Scott, B. L.; Boncella, J. M. Preparation and Reactivity of the Versatile Uranium(IV) Imido Complexes $U(NAr)Cl_2(R_2bpy)_2$ (R = Me, ^{t}Bu) and $U(NAr)Cl_2(tppo)_3$. *J. Inorg. Chem.* **2014**, dx.doi.org/10.1021/ic5014208.
11. Jilek, R. E.; Spencer, L. P.; Lewis, R. L.; Scott, B. L.; Hayton, T. W.; Boncella, J. M. A Direct Route to Bis(imido)uranium(V) Halides via Metathesis of Uranium Tetrachloride. *J. Am. Chem. Soc.* **2012**, *134*, 9876-78.
12. Hayton, T. W. ; Boncella, J. M.; Scott, B. L.; Palmer, P. D.; Batista, E. R.; Hay, P. J. Exchange of an Imido Ligand in Bis(imido) Complexes of Uranium. *J. Am. Chem. Soc.* **2006**, *128*, 12622-23.
13. Denning, R. G. Electronic Structure and Bonding in Actinyl Ions and Their Analogs. *J. Phys. Chem.* A **2007**, *111*, 4125.
14. Spencer, L. P.; Yang, P.; Scott, B. L.; Batista, E. R.; Boncella, J. M. Imido Exchange in Bis(imido) Uranium(VI) Complexes with Aryl Isocyanates. *J. Am. Chem. Soc.* **2008**, *130*, 2930.
15. Jilek, R.; Tomson, N. C.; Scott, B. L.; Boncella, J. M. [2+2] Cycloaddition Reactions at Terminal Imido Uranium(IV) Complexes to Yield Isolable Cycloadducts. *Inorg. Chim. Acta.* **2014**, *422*, 78-85.

Actinide Research Quarterly

Actinide Research Quarterly is published by Los Alamos National Laboratory and is a publication of the Glenn T. Seaborg Institute for Transactinium Science, a part of the National Security Education Center. ARQ highlights research in actinide science in such areas as process chemistry, metallurgy, surface and separation sciences, atomic and molecular sciences, actinide ceramics and nuclear fuels, characterization, spectroscopy, analysis, and manufacturing technologies.

Los Alamos National Laboratory, an affirmative action/equal opportunity employer, is operated by Los Alamos National Security, LLC, for the National Nuclear Security Administration of the US Department of Energy under contract DE-AC52-06NA25396.

LA-UR-15-24862

Los Alamos
NATIONAL LABORATORY
EST. 1943

NNSA
National Nuclear Security Administration